CONF-8205157--2

CONF-8205157--2

DE87 008461

GEOLOGIC CHARACTER OF TUFFS IN THE UNSATURATED ZONE AT YUCCA MOUNTAIN, SOUTHERN NEVADA

Robert B. Scott
Richard W. Spengler
Sharon Diehl
U.S. Geological Survey, MS 954
Denver Federal Center
Denver, CO 80225
A. R. Lappin
Sandia National Laboratories
Box 5800
Albuquerque, NM 87185
Michael P. Chornack
Fenix & Scisson
Box 498
Mercury, NV 89023

ABSTRACT

At Yucca Mountain, a potential site for a high-level nuclear waste repository on the Nevada Test Site in southern Nevada, evaluation of the geologic setting and rock physical properties, along with previous regional hydrologic studies, has provided background that can be used for construction of a preliminary conceptual hydrologic model of the unsaturated zone.

The 500-m-thick unsaturated portion of Yucca Mountain consists of alternating layers of two contrasting types of tuff. One type consists of highly fractured, densely welded, relatively nonporous but highly transmissive ash-flow tuffs. The other type consists of relatively unfractured, nonwelded, highly porous but relatively nontransmissive, argillic and zeolitic bedded tuffs and ash-flow tuffs. The contrast between these two sets of distinctive physical properties results in a stratified sequence best described as "physical-property stratigraphy" as opposed to traditional petrologic stratigraphy of volcanic rocks.

Superimposed on this layering are two sets of faults and fractures: one strikes north-northwest (N. 15° W. to N.

40° W.) and dips steeply (60°-90°) westward; the other strikes north-northeast (N. 5° E. to N. 35° E.) and also dips steeply westward. The north-northeast set constitutes the major Basin and Range style normal faults that separate the gently eastward-tilted major structural blocks of Yucca Mountain. The hanging-wall sides of these faults commonly exhibit increases in dip similar to rollover structures commonly related to listric faults. The north-northwest fracture set has the higher density, and the north-northwest fault set appears to have two directions of displacement. One is right-lateral slip perhaps related to the Las Vegas Valley and Walker Lane shear zones; the other is dip slip perhaps related to brittle drag behavior adjacent to the major north-northeast-striking faults.

The vast majority of recharge through the unsaturated zone is assumed to be vertical; the dominant migration may occur in fractures of densely welded tuffs and in the matrix of nonwelded tuff, but the mode of fluid flow in these unsaturated systems is undetermined. Limited lateral flow of recharge may occur at horizons where local perched water tables may exist above relatively nontransmissive zeolitized nonwelded tuffs. The pervasive north-northwest-striking fractures may control the direction of lateral flow of recharge, if any, in the unsaturated zone, and certainly that direction coincides closely with the observed southeasterly flow direction in the saturated zone under Yucca Mountain. Empirical evaluation of this conceptual hydrologic model has begun.

INTRODUCTION

The Nevada Nuclear Waste Storage Investigations project, administered by the Nevada Operations Office of the U.S. Department of Energy, is examining the feasibility of emplacing nuclear wastes in southern Nevada. As part of that effort, the U.S. Geological Survey (USGS) and Sandia National Laboratories (SNL), among other research groups, have participated in investigations of the geology, hydrology, geophysics, and rock properties of the thick sequence of silicic tuffs that occur within and contiguous to the Nevada Test Site (NTS) in Nye County, Nevada (Figure 1). These efforts augment more than 20 years of geologic research by the USGS at the NTS [1], within the southern part of the Great Basin subprovince. Site-specific investigations, carried out since 1978, have concentrated on the characterization of the 1.5- to 4 km-thick sequence of ash-flow tuffs and related rocks at Yucca Mountain (Figure 2). Recently, emphasis has been placed on the unsaturated zone

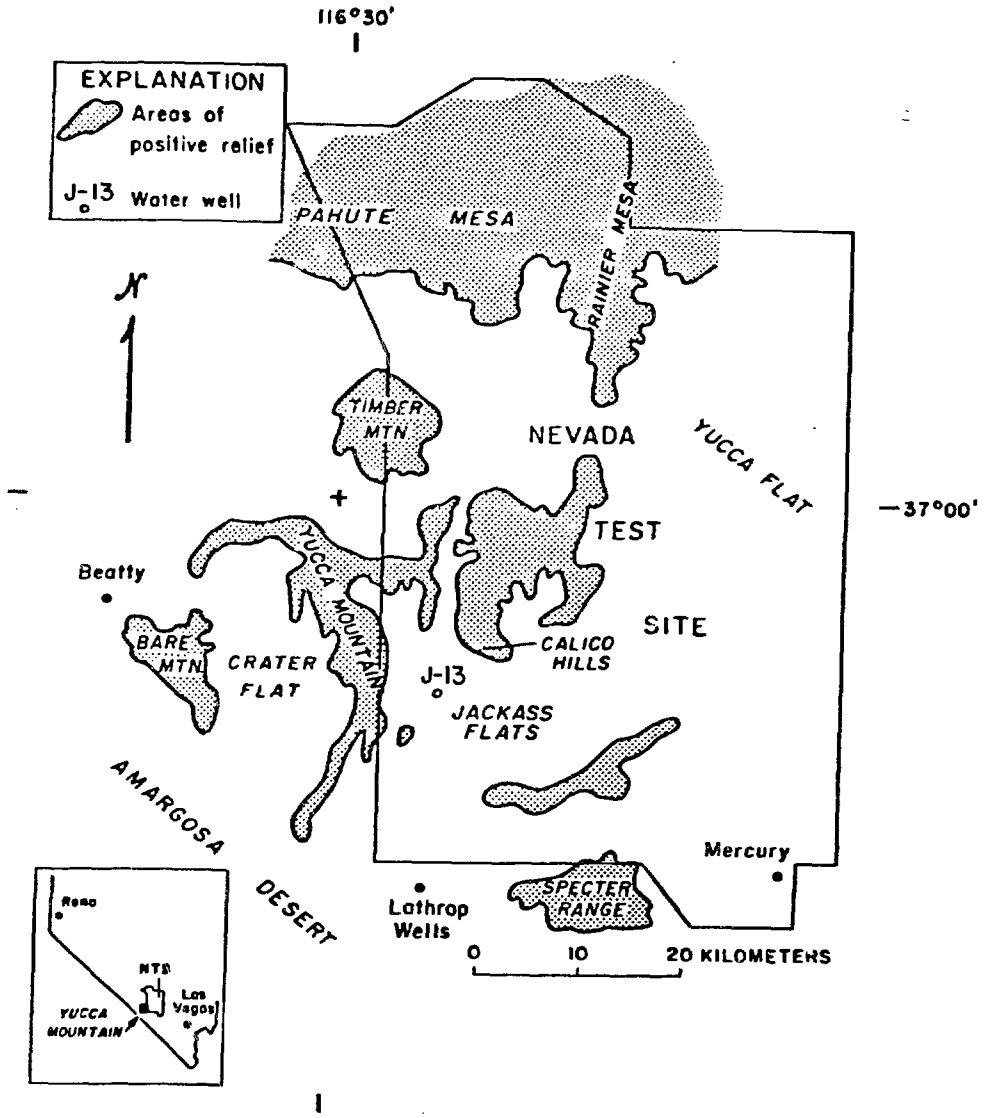

Figure 1. Location map. Index map at lower left shows the location of the Nevada Test Site (NTS) within Nevada, and the center shows an expansion of the southwest portion of the NTS.

which is some 500 to 800 m thick under Yucca Mountain. The sequence within the unsaturated zone consists of a wide range of contrasting rock types including densely welded devitrified and vitric ash-flow tuffs, nonwelded vitric ash-flow tuffs, vitric bedded tuffs, nonwelded zeolitized and argillized ash-flow tuffs, and zeolitized and argillized bedded tuffs.

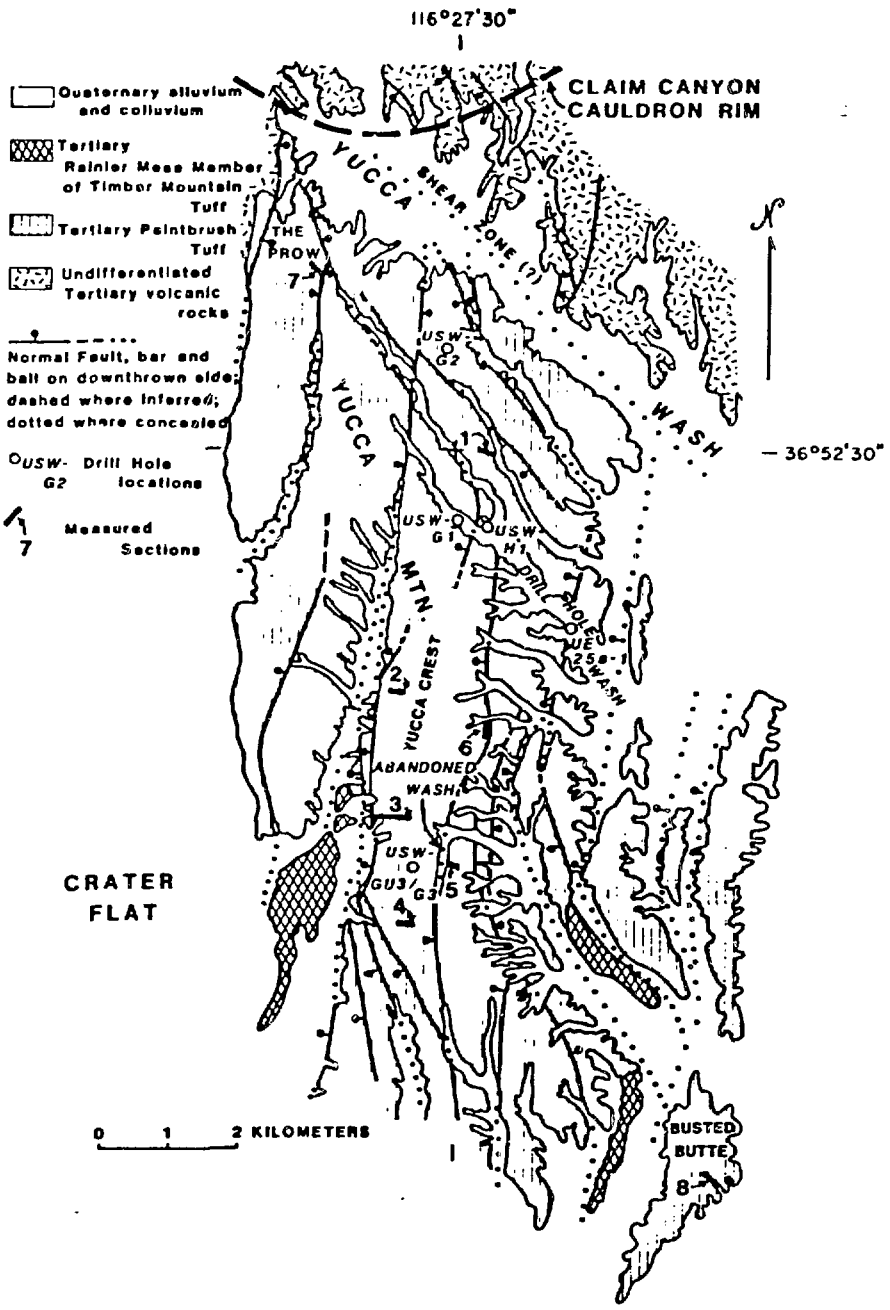

Figure 2. Geologic map of central Yucca Mountain generalized from the work of Christiansen and Lipman [3] and Lipman and McKay [4]; and modified based on results of recent detailed mapping. Exact boundaries of the area of the potential repository within this map area are not drawn because data are still being collected that may affect the most favorable boundaries.

This chapter deals principally with the geologic character and rock properties that potentially affect the hydrology of the unsaturated zone. Because the static water level at Yucca Mountain is 500 to 800 m below the surface, the unsaturated zone provides a thick sequence of welded and nonwelded tuffs for possible storage of nuclear waste. Several reasons for serious consideration of the unsaturated zone for waste storage in the Great Basin subprovince were reviewed by Winograd [2]; although the basic logic outlined by Winograd emphasized burial in thick alluvium, his logic can be extended to the unsaturated zones of fractured, densely welded ash-flow tuffs. This extension of logic includes: 1) low recharge flux in arid climates; 2) movement of recharge through highly transmissive, thermally stable, densely welded tuffs; 3) thick unsaturated zones; 4) multiple barriers to radionuclide migration including retardation by sorptive zeolitic and argillic nonwelded tuffs; 5) favorable thermal loading; and 6) economic factors of relatively shallow burial.

Among the most critical parameters of nuclear waste isolation is the transport of radionuclides by ground water. Ground-water movement in the NTS region is largely a function of effective rock conductivities [5]. Factors that govern effective rock conductivities in an ash-flow tuff are numerous; several factors produce matrix conductivity: At the time an ash flow is initially emplaced, the glass shard matrix becomes flattened by the welding process, provided the interior of the ash flow is at temperatures in excess of 500°C. This welding process creates an inverse relation between glass shard porosity and the degree of welding, but a positive relation between bulk density and the degree of welding. In the process of squeezing trapped gases from between the shards, gas-rich portions of ash-flow tuffs may develop gas pockets called lithophysal cavities. Most ash-flow tuffs consist of intercalated tongue-like sheets resulting from a series of magmatic pulses; if extruded over a short period at high temperatures, these individual sheets effectively weld into one sheet with decreases in degree of welding observable only at the margins of the sheet. Such sheets are called simple cooling units [6]. Alternatively, cooling periods of sufficient duration between individual magmatic pulses may cause decreases in the degree of welding within the interior of the cooling unit. Such ash-flow sheets are called compound cooling units. Within either compound or simple cooling units, small pore sizes (less than tens of micrometers) and assumed high tortuosities, particularly in the densely welded interiors of ash flows, create very low matrix conductivities: typical values are about 10^{-4} cm/s for vitric nonwelded tuffs and about 10^{-9}

cm/s for densely welded tuffs [5].

Superimposed upon this cooling-unit framework and matrix conductivity are the effects of 1) devitrification in the slowly cooled interiors and vapor-phase crystallization in the partially welded margins, 2) vertical extension joints produced during cooling, 3) alteration to secondary phases, by reaction with pore waters to form zeolites and clays, concentrated in less welded portions of the cooling units, and 4) faults and joints related to tectonic events. The term fracture is used to refer to any crack with undetermined offset; those without offset are joints, and those with known offset are faults. A wide variety of fracture densities, attitudes, and apertures are formed as a function of the behavior of a particular rock type to its stress environment. Also, a variety of minerals may fill part or all of the fractures.

The net effect of all these processes, discussed in the paragraph above, is to alter drastically the effective rock conductivities. Highly fractured, densely welded tuffs have effective hydraulic conductivities about 5 or 6 orders of magnitude higher than their matrix hydraulic conductivities [5]. Nonwelded vitric tuffs have effective hydraulic conductivities only about 1 order of magnitude higher than matrix hydraulic conductivities, but zeolitized or argillized nonwelded tuffs have effective hydraulic conductivities 1 to 4 orders of magnitude higher than matrix hydraulic conductivities [5,7]. A note of caution should be added here because these effective hydraulic conductivities were measured in saturated rocks [5]; those for the unsaturated rocks of interest at Yucca Mountain may be significantly lower and may be related to the degree of saturation. These differences emphasize the need to evaluate rock properties in their stratigraphic and structural framework. Thus, the principal objective of this paper is to characterize qualitatively those rock-mass properties that may affect the hydrology of the unsaturated zone at Yucca Mountain.

PREVIOUS GEOLOGIC INVESTIGATIONS

Prior to nuclear waste storage investigations, geologic research and exploration within the immediate vicinity of Yucca Mountain were limited to reconnaissance geologic quadrangle mapping [3-4]. Several summaries of the volcano-tectonic history of the NTS region that specifically address the origin of ash-flow tuffs exposed at Yucca Mountain have also been published [8-10]. Regional tectonic and structural relationships for the NTS and vicinity have been summarized by Carr [11].

Stratigraphic Framework

Although less than 2 km of Miocene (12.5 to 14 m.y.-old) ash-flow tuffs with minor lavas and bedded tuffs have been penetrated by drilling with continuous core recovery [12-14] (Florian Maldonado, USGS, and Sarah Koether, Fenix & Scisson (F&S), written commun., 1982), geophysical evidence suggests that a sequence of tuffaceous rocks between 1.5 and 4 km thick overlies a pre-Cenozoic basement under central Yucca Mountain [15]. The volcanic sequence beneath Yucca Mountain is shown on a north-south cross section (Figure 3). Four major ash-flow tuffs have been been penetrated by

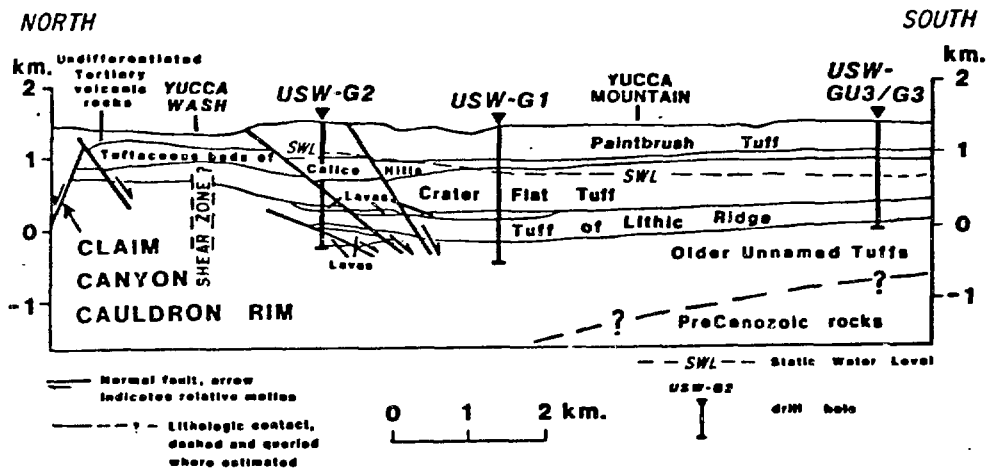

Figure 3. Generalized north-south geologic section through Tertiary volcanic strata under Yucca Mountain. SWL marks the static water level. Horizontal and vertical scales are the same. The zero depth is mean sea level.

drilling. These tuffs are listed in ascending order: 1) The informal tuff of Lithic Ridge (300±m thick) (W. J. Carr, USGS, F. W. Byers, Los Alamos National Laboratory (LANL), and Paul Orkild, USGS, written commun., 1982) consists of a partially to moderately welded, rhyolitic compound cooling unit. 2) The Crater Flat Tuff includes three rhyolitic ash-flow tuff members. The basal unit is the informal Tram unit (300±m thick), which consists of a partially to moderately welded, compound cooling unit. The middle member is the Bullfrog Member (200±m thick), which consists of a partially to densely welded, compound cooling unit. The upper member is the Prow Pass Member (100±m thick), which consists of a partially welded, compound cooling unit (W. J. Carr, USGS,

F. W. Byers, LANL, and Paul Orkild, USGS, written commun., 1982; R. B. Scott, USGS, and Mayra Castellanos, F&S, written commun., 1982). All three members are considered to have erupted from a caldera complex now buried below Crater Flat several kilometers to the west of Yucca Mountain [16] (W. J. Carr, USGS, F. W. Byers, LANL, and Paul Orkild, USGS, written commun., 1982). 3) A nonwelded sequence of rhyolitic ash-flow tuffs and bedded tuffs (30 to 275 m thick) is informally called the tuffaceous beds of Calico Hills [12] (Florian Maldonado, USGS, and Sarah Koether, F&S, written commun., 1982; R. B. Scott, USGS, and Mayra Castellanos, F&S, written commun., 1982). 4) The uppermost formation, the Paintbrush Tuff, here consists largely of two major ash-flow tuffs, the Topopah Spring Member (300±m thick) and the Tiva Canyon Member (100±m thick). Both the Topopah Spring and Tiva Canyon Members were erupted from the Claim Canyon Cauldron about 2 km north of Yucca Mountain [8]. Both the Topopah Spring and the Tiva Canyon Members largely consist of moderately to densely welded tuff, and they are both compositionally zoned from the high-silica rhyolites that form their basal and central portions to quartz latites that form densely welded caprocks near the top of each member [17,8]. In the stratigraphic interval between the Topopah Spring and Tiva Canyon Members, two minor members of the Paintbrush Tuff, the Pah Canyon and Yucca Mountain Members, are present at the north end of Yucca Mountain as distal edges of nonwelded to moderately welded sheets that pinch out toward the south and east within the central portion of Yucca Mountain [12] (Florian Maldonado, USGS, and Sarah Koether, F&S, written commun., 1982). Where these two members become too thin to map, they are lumped together with unnamed bedded tuffs. Although the Paintbrush Tuff is the youngest (12.5 to 13.1 m.y. old) ash-flow tuff to cover the entire Yucca Mountain area, the 11.3-m.y.-old Rainier Mesa Member of the Timber Mountain Tuff was locally ponded in post-Paintbrush Tuff structural depressions, covering portions of the normal faults that delineate the major structural blocks of the mountain (Figure 2).

The remainder of this chapter considers the characteristics of those units that occur above the static water level at Yucca Mountain. The static water level (Figure 3) within Yucca Mountain is located near the base of the Paintbrush Tuff at drill hole USW-G2, near the base of the tuffaceous beds of Calico Hills at USW-G1, and within the Crater Flat Tuff at USW-GU3/G3 [12] (Florian Maldonado, USGS, and Sarah Koether, F&S, written commun., 1982; R. B. Scott, USGS, and Mayra Castellanos, F&S, written commun., 1982).

Structural Framework

Paleozoic strata are not exposed within 15 km of Yucca Mountain, though seismic refraction (W. D. Mooney, USGS, written commun., 1982) and gravity data [15] suggest that Paleozoic rocks may be present under 1.5 to 4 km of volcanic strata. As no drilling has penetrated these rocks under Yucca Mountain, their character must be extrapolated from nearby exposures in the Specter Range, Calico Hills, and Bare Mountain (see Figure 1) [18]. Paleozoic rocks in these localities have been deformed by complex folding and thrust faulting during formation of the late Mesozoic Sevier orogenic belt [19-20]. Ambiguities inherent in these regionally complex structures do not allow reliable projections of either structures or lithologies under Yucca Mountain. Paleozoic carbonate or clastic rocks are likely to form the subvolcanic rocks. Regional interpretations of these Mesozoic structures vary [11,20] (M. D. Carr, USGS, oral commun., 1982), and possible structures under Yucca Mountain include upper or lower plates of regional overthrusts, low-angle gravity-controlled fault complexes, or broad folds. Because Paleozoic rocks are regionally important aquifers and aquitards in the southern Great Basin [5], penetration into subvolcanic rocks remains one of the ultimate objectives of the USGS investigations at Yucca Mountain.

Regionally, three types of Cenozoic structures exist: 1) Basin and Range style faults, 2) major strike-slip fault zones, and 3) volcano-tectonic structures. Relative to the heterogeneous and complex Cenozoic structure common in surrounding areas, the structure at Yucca Mountain appears uncomplicated. As exposures of pre-Paintbrush Tuff rocks are sparse, the apparent structural simplicity of Yucca Mountain may be misleading to some degree. However, structural data from cores to depths of nearly 2 km do not suggest the presence of structural styles or complexities not apparent on the surface. Pre-Paintbrush Tuff Tertiary structures below the 2 km depths explored by drilling probably do exist beneath Yucca Mountain, as suggested by the gravity and magnetic gradients [15] (G. D. Bath, USGS, written commun., 1982).

As shown in quadrangle maps [3,4], Yucca Mountain itself is broken by several major north-northeast-striking and generally westward dipping Basin and Range style normal faults with tens to hundreds of meters of vertical displacement, forming blocks tilted gently eastward. In general, these faults decrease in displacement and density toward the north (Figure 2). Basin and Range style normal faulting

began prior to volcanism [21,11] and continued during most of the major eruptive activity; apparently, few if any faults formed after volcanism ceased, although relatively minor additional displacements have occurred locally on preexisting faults during the last few million years. Regional evidence of Quaternary faulting in response to a minimum principal horizontal stress direction of about N. 50° W. has been reviewed by Carr [11]. Direct evidence of this type of faulting at Yucca Mountain is not reported in previous studies, but has been found by recent mapping (W. J. Carr, USGS, oral commun., 1982). The original geologic mapping at Yucca Mountain [3,4] did not identify volcanotectonic structures associated with the Crater Flat Tuff; however, such structures are now believed to exist in the vicinity of Crater Flat [15].

Hydrologic Framework

Extensive summaries of the NTS region and local hydrology have been made [5,7,22-24], but no details were previously available concerning the Yucca Mountain area. The regional water table is commonly 500 to 800 m deep and has a south and southwest flow direction toward the Amargosa Desert in most of the region. However, in local areas considerable variation is observed such as the southeast flow direction under Yucca Mountain. The principal aquifers in the NTS region are Paleozoic carbonate rocks and highly fractured Tertiary densely welded ash-flow tuffs. The major aquitards are Paleozoic clastic rocks and Tertiary zeolitized or argillized nonwelded tuffs. For example, a few kilometers east of Yucca Mountain in Jackass Flats (Figure 1), where the Topopah Spring Member is below the water table, the densely welded tuff is an aquifer in well J-13 [24,5]. Matrix and effective hydraulic conductivities of the major rock types found within ash-flow tuffs at the NTS are given in Table I.

GEOLOGIC CHARACTER OF THE UNSATURATED ZONE

Physical-Property Stratigraphy

The movement of fluids through rock is fundamentally a physical process. For this reason, a stratigraphic framework designed to emphasize potential differences in the hydrologic character among strata should be based upon rock physical properties. Petrologic differences, usually identified by phenocryst ratios, are traditionally used to

Table I. Hydraulic Conductivities of Tuffaceous Aquifers and Aquitards, NTS

Hydrologic Unit	Rock Type	Range of Matrix Hydraulic Conductivities[1] (cm/s)	Range of Effective Hydraulic Conductivities[2] (cm/s)
Aquifer	Densely welded tuff[3]	3×10^{-10} to 10^{-8}	10^{-5} to 3×10^{-2}
Leaky Aquitard[4]	Nonwelded vitric tuff	10^{-4}	$\sim 10^{-3}$
Aquitard	Nonwelded zeolitized tuff	2×10^{-9} to 3×10^{-5}	10^{-6} to 10^{-4}
Aquitard	Nonwelded argillized tuff	10^{-10} to 2×10^{-5}	10^{-6} to 10^{-4}

[1]Upper range for welded tuff from page 34, lower range for welded tuff from Figure 18, and zeolitized and argillized tuff from Table 5 from Winograd and Thordarson [5].

[2]From Table 1 of Winograd and Thordarson [5] and Thordarson (USGS, written commun., 1965), and estimated from thicknesses of nonwelded vitric tuffs at margins of cooling units.

[3]Values for both devitrified and vitric densely welded tuff are included.

[4]Term used by Winograd and Thordarson [5].

define stratigraphic breaks in sequences of ash-flow tuffs, but for the hydrologic and engineering concerns of a nuclear waste repository, physical property differences in porosity, bulk density, grain density, permeability, and degree of welding, along with the density and attitudes of fractures and faults, are the important features. To contrast these two different stratigraphic classification schemes, Figure 4 compares petrologic stratigraphy with a physical-property

stratigraphy based on the degree of welding in the sequence of rocks cored at holes USW-GU3/G3, -G1, and -G2 [12] (R. B. Scott, USGS, and Mayra Castellanos, F&S, written commun., 1982; Florian Maldonado, USGS, and Sarah Koether, F&S, written commun., 1982). The physical-property subdivisions shown in Figure 4 were produced by placing bedded tuffs and nonwelded to partially welded ash-flow tuffs into one category and moderately to densely welded ash-flow tuffs into a second category. The first category consists of relatively low-density rocks that tend to be more porous and less fractured than those in the second category, which consists of relatively high-density rocks that tend to be less porous and more fractured. In combination with structural data, physical-property stratigraphy, as expressed in Figure 4, is particularly useful for construction of conceptual hydrologic models. The variability in this physical-property stratigraphy from USW-GU3/G3 in the southern part of the Yucca Mountain region to USW-G2 in the northern part of the region is considerable, over a distance of only 8 km.

Detailed investigations of the physical properties of the Tiva Canyon Member of the Paintbrush Tuff were possible because of the excellent three-dimensional exposures of this member at Yucca Mountain. The Tiva Canyon Member is very similar in overall character to the less well exposed Topopah Spring Member. This similarity is supported by the observation that the physical properties of surface samples of the welded Tiva Canyon Member are comparable to those of core samples of the welded Topopah Spring Member [26-27]. In addition to studies of the more welded units, determinations of physical properties have been made for the bedded and nonwelded tuffs [28]. These physical property studies are augmented by petrological and chemical studies made at the Los Alamos National Laboratory [29], which describe the character of clay and zeolite alteration in both welded and nonwelded tuffs.

Mappable Zonations within the Tiva Canyon Member

Zonations within ash-flow tuffs, as defined by Smith [6], primarily reflect the effects of the thermal evolution of ash-flow tuffs; Lipman and others [17] discussed the origin of primary chemical zonations that reflect primary magmatic differences. Zonations used to study ash-flow tuffs at Yucca Mountain are recognized in the field by differences in groundmass devitrification, degree of welding, shape of eroded slopes, texture of weathered surfaces created by both surficial cracking and tectonic fracturing, lithophysal cavity abundance, lithic fragment abundance,

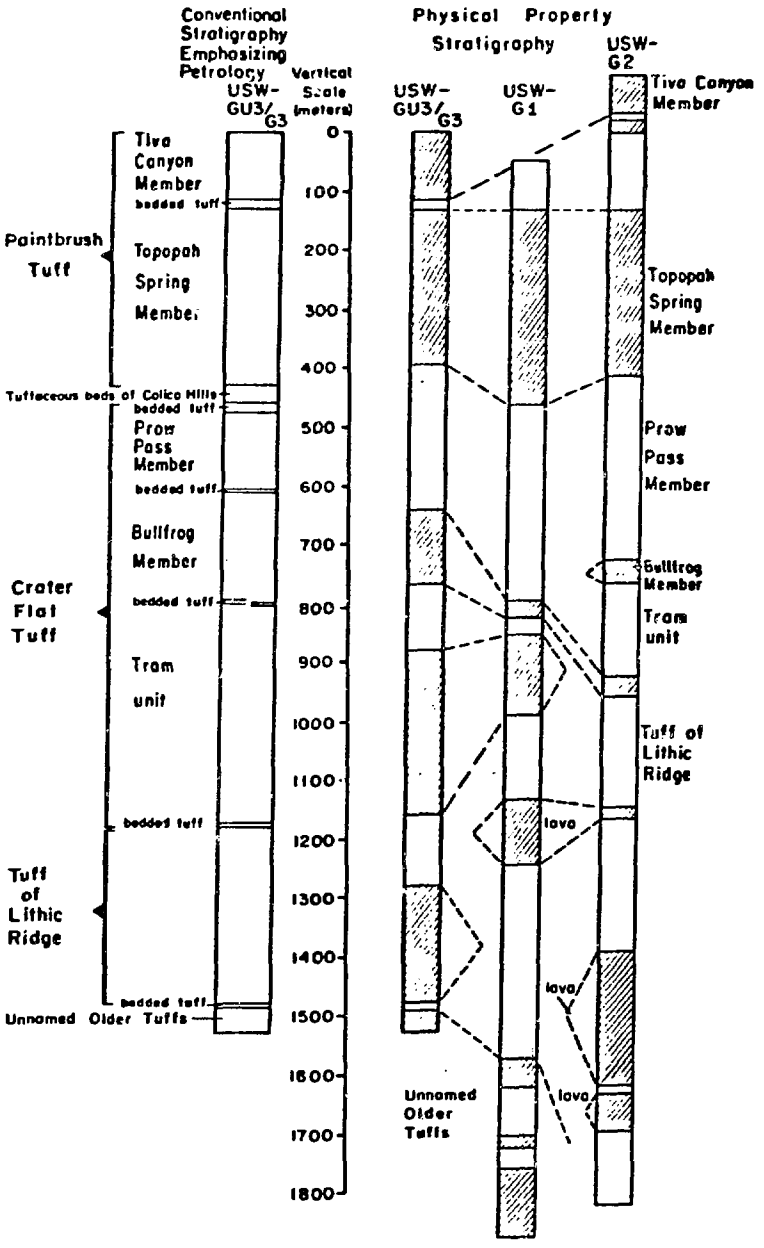

Figure 4. Comparison between stratigraphic units defined by petrologic criteria and those defined by physical-property criteria. The conventional stratigraphic nomenclature based upon petrologic criteria is given for drill hole USW-GU3/G3 on the left and the physical-property stratigraphies based on degree of welding for drill holes USW-GU3/G3, -G1, and -G2 are drawn in order toward the right. The conventional stratigraphic names

of major units are also listed on the far right for general reference but exact boundaries are not shown. The shaded zones are moderately welded to densely welded; unshaded are nonwelded to partially welded. BT = bedded tuff.

phenocryst ratios, presence of vapor-phase crystallization, and color. Besides forming stratigraphic horizons particularly valuable for recognition of small faults, these zones provide a stratigraphic framework for comparison with the physical properties of the rocks. A fence diagram of this zonation in the Tiva Canyon Member is shown in Figure 5; each station of the fence diagram is a measured section (located in Figure 2) where samples were also collected for physical- property studies. The informal field terms for these zones are used on the fence diagram.

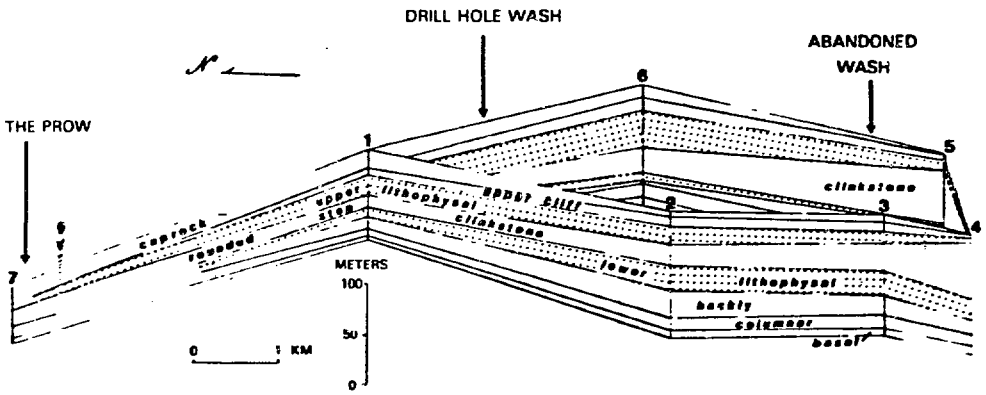

Figure 5. Generalized zonation within the Tiva Canyon Member. The rounded step zone grades laterally into the clinkstone zone. Measured section numbers are located on Figure 2.

Bulk Density, Porosity, and Grain Density

Measured dry bulk densities, matrix porosities, and grain densities for different zones of the Tiva Canyon Member are shown on Table II. Similar values have been reported for these physical properties in the core of drill hole UE25a-1 [25]. The interdependence of dry bulk density and matrix porosity is shown in Figure 6; as expected, dry bulk density increases and porosity decreases as welding increases. Different degrees of welding should not be defined by specific porosity or density limits because considerable variation in both total porosity (including

Table II. Physical Properties of the Tiva Canyon Member of the Paintbrush Tuff, Yucca Mountain
(Analyses by Terra Tek, Inc., Salt Lake City)

Measured Section Sample Number	Height above base (m)	Zone	Dry bulk density[1] (g/cm^3)	Grain density[2] (g/cm^3)	Matrix porosity[3] (percent)
YTC1-12	88.3	caprock	2.24	2.50	10.4
YTC1-11	80.3	caprock	1.77	2.51	29.5
YTC1-10	72.2	caprock	1.99	2.48	19.8
YTC1-9	66.1	upper cliff	2.11	2.50	15.6
YTC1-8	59.1	upper lithophysal	2.16	2.53	14.6
YTC1-7	46.8	upper lithophysal	2.10	2.45	14.3
YTC1-6	36.9	rounde step	2.20	2.45	10.2
YTC1-5	29.2	lower lithophysal	2.21	2.47	10.5
YTC1-4	18.4	hackly	2.29	2.47	7.3
YTC1-3	10.8	columnar	2.14	2.46	13.0
YTC1-2	6.1	columnar	2.17	2.47	12.1
YTC1-1	2.3	basal	1.36	2.38	42.9
YTC2-15	124.0	caprock	1.89	2.47	23.5
YTC2-14	122.1	caprock	1.82	2.53	28.1
YTC2-13	119.0	upper cliff	1.96	2.52	22.2
YTC2-12	109.8	upper cliff	2.17	2.46	11.8
YTC2-11	93.7	upper lithophysal	2.18	2.47	11.7
YTC2-10	86.0	rounded step	2.23	2.44	8.6
YTC2-9	78.4	rounded step	2.24	2.44	8.2
YTC2-8	71.4	rounded step	2.18	2.51	13.2
YTC2-7	63.0	lower lithophysal	2.24	2.44	8.2
YTC2-6	49.9	lower lithophysal	2.18	2.40	9.2
YTC2-5	39.2	hackly	2.34	2.52	7.1
YTC2-4	23.0	hackly	2.29	2.45	6.5
YTC2-3	16.9	columnar	2.26	2.44	7.4
YTC2-2	10.0	columnar	2.01	2.43	17.3
YTC2-1	3.8	basal	1.27	2.35	46.0
YTC3-14B	116.5	caprock	1.97	2.55	22.7
YTC3-14A	102.8	uppercliff	2.17	2.52	13.9
YTC3-13B	66.5	clinkstone	2.20	2.48	11.3
YTC3-13A	47.6	lower lithophysal	2.29	2.48	7.7
YTC3-12B	38.5	hackly	2.29	2.45	6.5
YTC3-12A	35.4	hackly	2.31	2.46	6.1
YTC3-11A	25.3	hackly	2.34	2.47	5.3
YTC3-10C	19.2	columnar	2.36	2.53	6.7
YTC3-10B	12.2	columnar	2.36	2.52	6.3
YTC3-10A	9.2	columnar	2.26	2.39	5.4
YTC3-9D	7.6	basal	2.14	2.43	11.9
YTC3-9C	3.0	basal	1.56	2.31	32.5
YTC3-9B	2.1	basal	1.32	2.37	44.3
YTC3-9A	0.0	basal	1.19	2.34	49.3

Table II. Physical Properties--Continued

Measured Section Sample Number	Height above base (m)	Zone	Dry bulk density[1] (g/cm^3)	Grain density[2] (g/cm^3)	Matrix porosity[3] (percent)
YTC4-8B	107.6	caprock	1.92	2.55	24.7
YTC4-8A	100.0	upper lithophysal	2.17	2.40	9.6
YTC4-7A	94.5	lower cliff	2.27	2.50	9.2
YTC4-6C	89.0	clinkstone	2.09	2.50	16.4
YTC4-6B	74.0	clinkstone	2.12	2.50	15.2
YTC4-6A	49.5	clinkstone	2.29	2.56	10.5
YTC4-5A	41.0	lower lithophysal	2.28	2.48	8.1
YTC4-4B	32.0	hackly	2.38	2.54	6.3
YTC4-4A	26.0	hackly	2.31	2.53	8.7
YTC4-3B	12.5	columnar	2.32	2.47	6.2
YTC4-3A	11.0	columnar	1.97	2.34	15.8
YTC4-2B	6.0	basal	1.51	2.49	39.4
YTC6-7B	103.3	caprock	1.98	2.51	21.1
YTC6-7A	78.0	upper cliff	2.16	2.49	13.3
YTC6-6B	52.5	upper lithophysal	2.14	2.51	14.7
YTC6-6A	42.4	upper lithophysal	2.12	2.51	15.5
YTC6-5B	30.4	clinkstone	2.32	2.50	7.2
YTC6-5A	16.7	clinkstone	2.30	2.52	8.7
YTC6-3A	10.6	lower lithophysal	2.26	2.52	10.3
YTC6-2A	8.5	hackly	2.32	2.53	8.5
YTC6-1B	3.7	columnar	2.34	2.51	6.3
YTC6-1A	0.0	columnar	2.32	2.48	6.5

[1]Dry bulk density calculated using volume of sample based on immersion; external lithophysal cavities are generally not evident in these data.

[2]Calculated by powdered pycnometer method.

[3]Calculated value, based on the formula: percent porosity = (grain density - dry bulk density)/grain density; therefore, lithophysal porosity generally is not included in these data.

lithophysal porosity) and matrix porosity, are common at constant degree of welding. Explanations for these variations include the presence of secondary mineralization, vapor-phase crystallization, and formation of lithophysal cavities.

Small shifts in the porosity-dry bulk density relationship shown in Figure 6 are not related to the degree of welding, but instead are related to small changes in grain density. The vitric basal portion (Figures 6 and 7) has the lowest average grain density within the Tiva Canyon Member (2.38 ± 0.06 g/cm^3). This is the same value reported for the vitric portion of the Topopah Spring Member in drill hole USW-G1 [26]. The average grain density within the partially vitric columnar zone of the Tiva Canyon Member is 2.46 ± 0.06

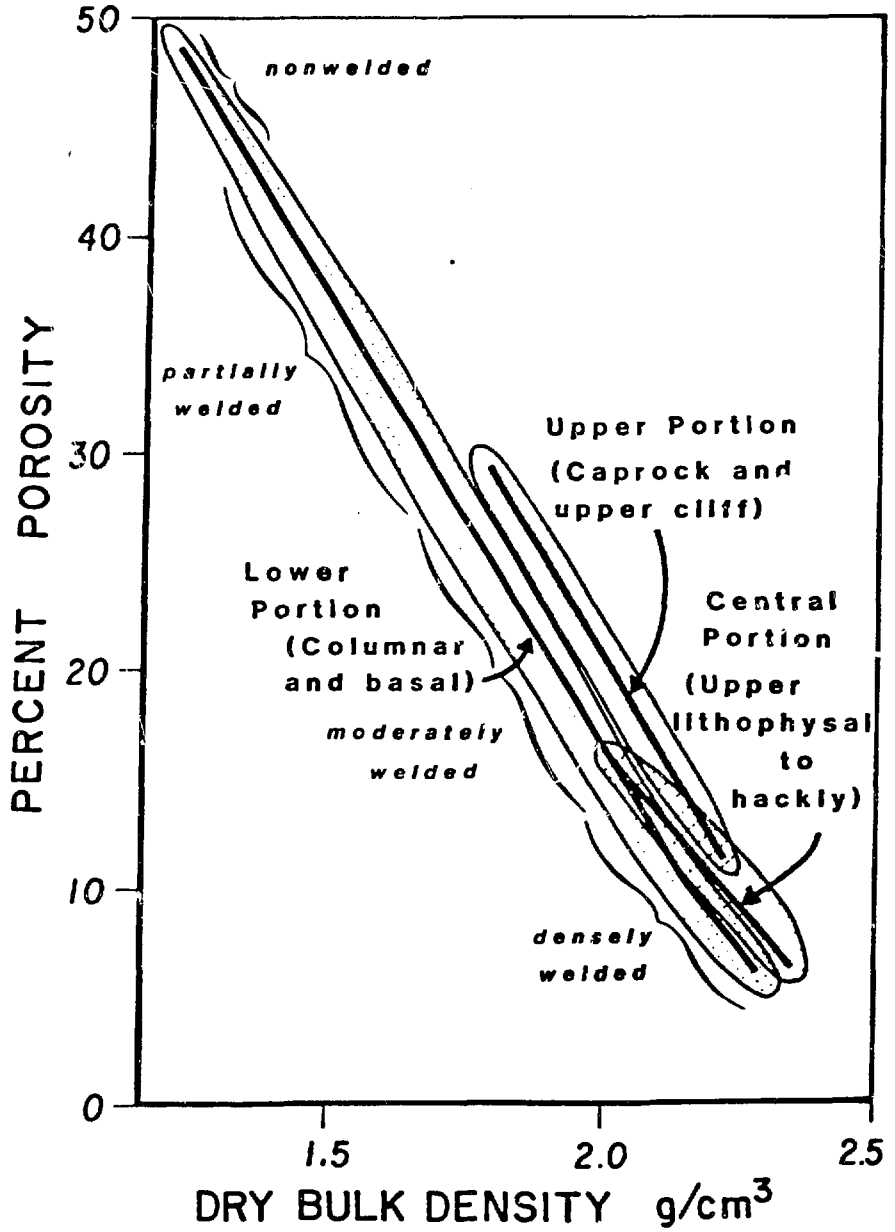

Figure 6. Relations between dry bulk density, matrix porosity, and degree of welding of the Tiva Canyon Member. The central portion includes the devitrified zones: the hackly, lower lithophysal, clinkstone, and upper lithophysal zones. Brackets show the general regions typical of rocks of different degrees of welding.

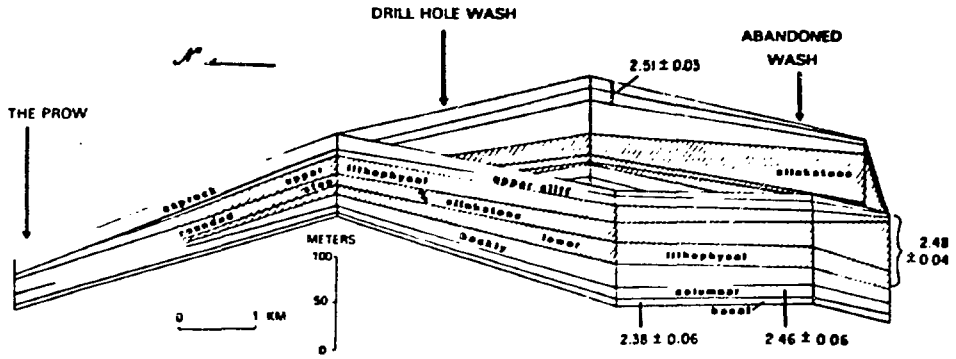

Figure 7. Grain density (g/cm^3) correlation with stratigraphic zones in the Tiva Canyon Member, Paintbrush Tuff.

g/cm^3, within the completely devitrified central portion is 2.48 ± 0.04 g/cm^3, and within the upper cliff and caprock zones is 2.51 ± 0.03 g/cm^3. The grain densities in the Tiva Canyon Member reported here are significantly lower than those reported for the devitrified portions of the Topopah Spring Member, which average 2.55 g/cm^3 [26]. Similar results were also obtained in the physical property studies of ash-flow tuffs in the Timber Mountain Caldera region (W. J. Carr, USGS, written commun., 1966).

Thus, a consistent trend of increasing grain density exists from the partially devitrified columnar zone upward through the devitrified central zones to the devitrified upper cliff and caprock zones, consistent with the offsets of curves in Figure 6. Several explanations for this trend can be given. First, the increase in average grain density of the partially devitrified columnar zone relative to the vitric basal zone is caused by the greater density of devitrification products, quartz, tridymite, cristobalite, and feldspar, compared to volcanic glass in the vitric zone. Second, higher densities in the central devitrified portion between the columnar and the upper cliff zones are also related to the greater densities of devitrified phases; the increase of grain density near the top of the central portion, specifically in the upper lithophysal zone, may be related, in part, to an increase in the phenocryst content from about 3 percent in the lower zones to about 6 percent in the upper lithophysal zone. Third, the greatest average grain densities, those found in the upper cliff and caprock zones, are probably related to two factors, an increase in phenocryst content to about 15 percent and the more mafic rock composition of those zones. Still another source of grain density variation within the devitrified portion of

the unit may be the ratios of silica polymorphs and feldspar; in particular, the grain densities of cristobalite (2.33 g/cm^3) and tridymite (2.26 g/cm^3) are significantly lower than that of quartz (2.65 g/cm^3). However, there is almost no quartz in the devitrification products in the Tiva Canyon Member, and the feldspar/silica polymorph ratio is essentially constant (Dave Bish, LANL, written commun., 1982). The presence of abundant quartz in the devitrification products of the Topopah Spring Member is consistent with the higher densities in the devitrified portion of that unit.

Devitrification

The devitrification textures evident in thin sections are also related to zones mapped in the field, and probably explain many of the differences in the character of weathered surfaces. For example, the hackly zone (see Figure 7) weathers to centimeter-sized irregular fragments, in contrast to the overlying clinkstone zone, which forms meter-long, smooth, conchoidally fractured blocks; field relationships do not suggest an explanation for this difference in surface characteristics. In thin section, however, the devitrification texture within the hackly zone consists of short, finely fibrous spherulitic patches (Figure 8a), while that in the clinkstone zone consists of long, coarsely fibrous to granophyric textures which both obscure and cross glass shard boundaries, forming a more uniform three-dimensional intergrowth (Figure 8b). The devitrification textures in the upper portions of the clinkstone zone and in the upper cliff and caprock zones are increasingly coarser granophyric with gradational contacts. The columnar zone has an almost unaltered flattened glass shard axiolitic texture that gradationally becomes devitrified toward the top of the zone. The basal zone has partially flattened shards with a hydrated(?) rim. The boundaries between these devitrification textures approximately follow the mapped zone boundaries (Figure 9).

Because these differences should affect the means by which these units fracture after devitrification, a correlation between devitrification zones and the density of fractures is expected. In drill hole USW-GU3/G3 where core was recovered from the Tiva Canyon Member, the calculated density of fractures in the densely welded portion of the unit is calculated to be 14 fractures/unit m^3 in the upper lithophysal zone, 22 fractures/unit m^3 in the clinkstone zone, 22 fractures/unit m^3 in the lower lithophysal zone, 26 fractures/unit m^3 in the hackly zone, and 21 fractures/unit

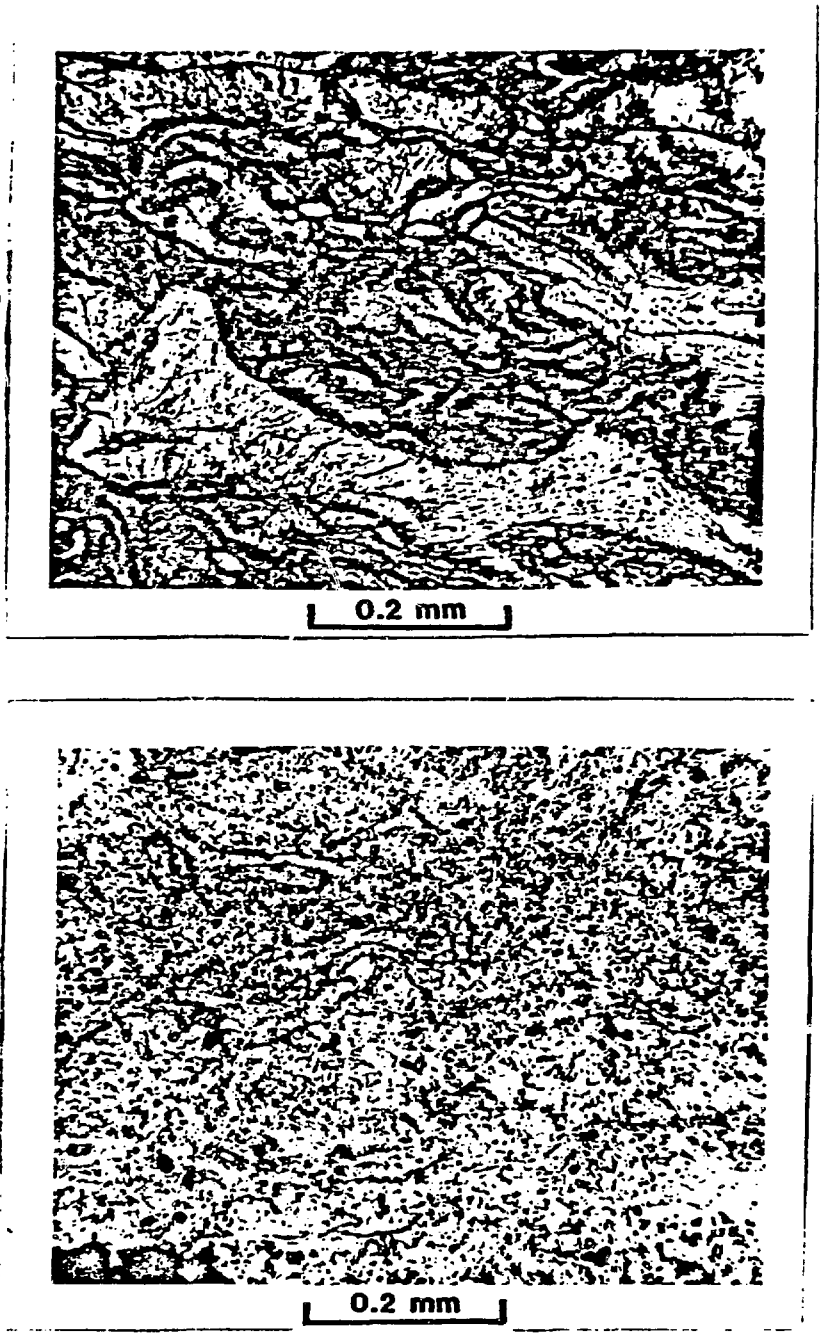

Figure 8. Photographs of thin sections of devitrified textures in the Tiva Canyon Member in the (a) hackly zone and (b) clinkstone zone. The glass shard texture is more distinct in the hackly zone but partially destroyed in the clinkstone zone.

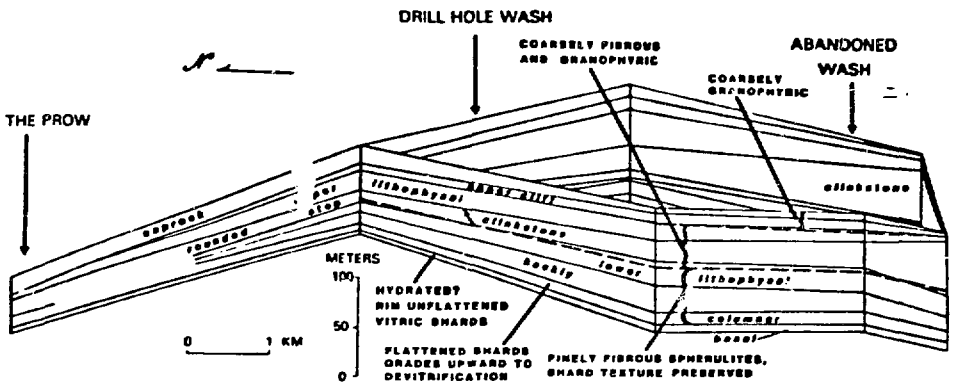

Figure 9. Stratigraphy of devitrification textures in the Tiva Canyon Member, Paintbrush Tuff. The dashed lines mark contacts between devitrification zonations that do not coincide with zone boundaries.

m^3 in the columnar zone. The partially welded caprock zone of the Topopah Spring Member has a fracture density of about 18 fractures/unit m^3 and should be representative of the unsampled portion of the Tiva Canyon caprock zone (an explanation of the fracture density units and calculation follows in a discussion of fractures). It may be significant that the hackly zone, with fine spherulitic devitrification textures, has the highest fracture density and that the upper lithophysal zone has the lowest fracture density, though it is apparent that zones of approximately the same degree of welding have approximately the same density of fracturing, in spite of variations in devitrification texture and lithophysal content. One exception to this general rule is that the density of fractures within the densely welded vitrophyres is appreciably lower than the overlying devitrified portion; for example, the Topopah Spring vitrophyre has a density of 8.8 fractures/unit m^3.

In contrast, the partially welded to nonwelded base of the Tiva Canyon Member has only 9 fractures/unit m^3, and the underlying bedded tuffs and nonwelded tuffs have less than 1 fracture/unit m^3. Thus, devitrification textures and lithophysal content appear to have much less impact on fracture frequency than degree of welding and vitrophyres have intermediate fracture densities.

Lithophysal Zones

Zones containing abundant lithophysal cavities or gas pockets may significantly affect many of the physical prop-

erties of ash-flow tuffs. Several lithophysal zones occur in the compound cooling units of the Tiva Canyon and the Topopah Spring Members; these have been mapped and studied in measured sections of the Tiva Canyon Member (Figure 5) and studied in measured sections and core of the Topopah Spring Member (Figure 10). Field relationships of the lithophysal zones in the Tiva Canyon Member suggest that these zones are continuous sheets, and that each lithophysal zone represents a separate gas-rich eruptive pulse. Field and detailed petrographic evidence suggests that the Tiva Canyon Member actually consists of at least 8 eruptive pulses, only two of which were gas-rich. The somewhat more irregular pattern of lithophysal zones in the Topopah Spring Member shown in Figure 10 probably represents a series of

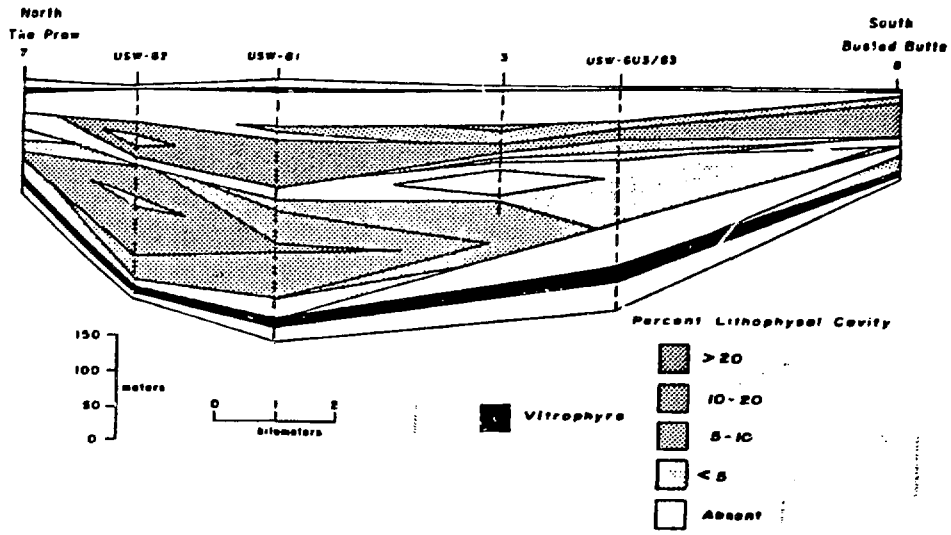

Figure 10. Lithophysal zonation in the Topopah Spring Member, Paintbrush Tuff. Locations of drill holes USW-G2, -G1, and -GU3/G3 and the measured sections 3, 7, and 8 are shown on Figure 2.

somewhat discontinuous stratigraphic tongues of gas-rich magmatic pulses that created lithophysal-rich horizons. At least 9 separate magmatic pulses can be recognized from petrographic evidence in the core from drill hole USW-GU3/G3 alone, and evidence for other stratigraphic units are found elsewhere in the field and in core [17] (R. B. Scott, USGS and Mayra Castellanos, F&S, written commun., 1982). Approximately 2 of these pulses were sufficiently gas-rich to produce lithophysal zones.

Lithophysal cavities consist of spherical to highly oblate voids ranging from less than 1 cm to as much as 30 cm

in maximum diameter. Surrounding these voids is a thin (∿1 mm thick) inner rim of vapor-phase crystals; cristobalite, tridymite, and alkali feldspar are common and plates of hematite, prisms of pseudobrookite, and needles of alkali amphiboles rare. Outside the vapor-phase rim itself is an outer rim of pale-colored altered rock matrix, commonly about 1 cm thick. In general, the alteration in this rim consists of the products of high-temperature mineralogical and chemical processes, but mixed layer clays are locally reported [29]. Lithophysal porosity varies from less than 1 percent to greater than 30 percent of the rock.

Obviously these cavities will influence effective hydraulic conductivities, especially in fractured zones; hydraulic tests of these specific zones are planned. Also these cavities, which are air-filled above the static water level, decrease rock thermal conductivities and bulk densities, and will alter rock-mass engineering or mechanical properties. Therefore, determination of the actual three-dimensional distribution of lithophysae within the Topopah Spring Member is being given high priority.

STRATIGRAPHIC CONTROL OF STRUCTURAL CHARACTER

Expression of Fracture Density

Knowledge of the character of fractures in a rock mass is essential to understanding or predicting its hydrologic character. Therefore, it is critical to express the attitude, distribution, and density of fractures properly when interpreting data collected either along an outcrop or in drill core. A critical problem in interpretation is created by fractures that intersect cores or traverses at angles less than 90°. In such a situation, the apparent fracture frequency per unit length along core or outcrop may be significantly less than the true fracture frequency per unit length perpendicular to the fracture set [30]. First, consider a simplified example where a core is cut by a set of parallel fractures that intersect the core axis at some angle less than 90°. In this example, the actual frequency of fractures per unit length in a direction perpendicular to the fracture set can be expressed by the relation:

$$F_c = [\sin A]^{-1} \cdot F_m$$

where F_c is the corrected fracture frequency, F_m is the apparent fracture frequency measured along the core axis, and A is the acute angle between the core axis and the fracture set (note: if the dip of the fracture is measured, use $[\cos \text{dip}]^{-1}$). This correction, in effect, determines the number of fractures that would have been encountered if the core were cut exactly perpendicular to the fracture

plane. In the real world of infinite fracture attitudes in a rock mass, fracture frequency per unit distance in all possible directions perpendicular to all fracture planes must be expressed. The locus of that unit distance in all directions geometrically generates a sphere. The sum of all the corrected fracture frequencies thus becomes the number of fractures within that spherical volume, that is, fracture density. The diameter of that sphere is the unit distance along which each fracture density is calculated. Because distance along a core or traverse increases by distance to the first power but volume increases by distance to the third power, the density of fractures must be expressed relative to a standard unit volume. In this work, the number of fractures per sphere with a unit volume of 1 m^3 is arbitarily chosen as the standard of comparison. Thus the unit distance, along which the fracture density is calculated, is the diameter of the sphere; for a sphere of 1 unit m^3, a unit distance of 1.24 meters must be used.

As an example, over an interval of 44.10 m of core in the highly fractured clinkstone zone of the Tiva Canyon Member, 179 fractures were observed. Using the angular correction described above, the sum of the calculated fracture frequencies along the entire interval would be about 800. The density of fractures within each unit volume of 1 m^3 is calculated by dividing the sum of the calculated fracture frequency in the entire interval by the number of standard volume diameters in the cored interval. The resulting number, 800 X 1.24/44.10 = 22, is the average number of fractures predicted within each sphere of 1 m^3 within the clinkstone zone.

Implicit within this statement is the acceptance of increasingly poor statistics as the angles between the fracture sets and the core axis or traverse direction become smaller. Also, the assumption is explicitly made that the total fracture density observed is representative of the entire stratigraphic zone from which data were collected. Thus, either the observed fractures or others with the same representative attitudes and densities are present throughout the sampled zone.

Recognition of Detailed Structural Features

Among the most critical factors for understanding hydrologic flow are the distribution, density, and attitude of minor faults. At Yucca Mountain, the recognition of minor faults presents a particularly difficult dilemma because the vast majority of exposures consists of one only cooling unit, the Tiva Canyon Member. To recognize faults

with less than about 3 m of displacement, detailed stratigraphic control must be available. Such control is provided by only a few horizons, such as the sharp transition at the top and base of the lower lithophysal zone and minor subhorizons within the columnar zone. In addition, the presence of tectonic breccia, gouge, slickensides, and abrupt changes in foliation attitudes were used to identify faults where insufficient stratigraphic control existed to reveal displacement. The resulting fault pattern is shown in Figure 11, and a detailed schematic east-west cross section in the vicinity of Abandoned Wash is shown in Figure 12.

Several important structural characteristics of Yucca Mountain are noted:

1) The shallow (5° to 7°) eastward dip of primary foliation typical of the crest of Yucca Mountain increases gradually toward Abandoned Wash, commonly to as much as 40°, and in a few instances over 70° (Figure 12). Where dips exceed approximately 10° to 20°, abundant small-displacement (less than 3 m), north-northwest-striking, westward-dipping, normal faults appear. These are present throughout the more highly tilted region around Abandoned Wash. The change in elevation of a stratigraphic horizon caused by the eastward dip is opposite in sense to the change in elevation caused by the offset along the west-dipping normal faults. Thus, in cross section, a single stratigraphic horizon and the connecting fault planes form a zig-zag pattern (Figure 12).

2) The abundance of north-northwest-striking (about N. 15° W.) faults decreases from Abandoned Wash northward where the steep foliation dips are absent.

3) North of Drill Hole Wash, right-lateral strike-slip faults are essentially parallel to and lie within several of the northwest-trending (N. 25°-40° W.) washes. These washes are also parallel to the trend of the dip direction of ash-flow tuffs. Therefore, the trends of these washes are probably the consequence of both faulting and runoff direction.

4) Numerous fractures are present on the surface of Yucca Mountain. Fractures can originate either from extensional stresses generated within the rock mass during cooling or from tectonic stresses applied to the rock mass after cooling. If cooling joints were exclusively present, only random fracture strikes would be observed; therefore, any departure from randomness is assumed be have a tectonic origin. The fracture densities and strikes along several traverses (corrected for fracture and traverse attitude as described above) are shown in rose diagrams in Figure 13. Six traverses were made, 5 in the Tiva Canyon Member and one in the tuffaceous beds of Calico Hills near The Prow. Where

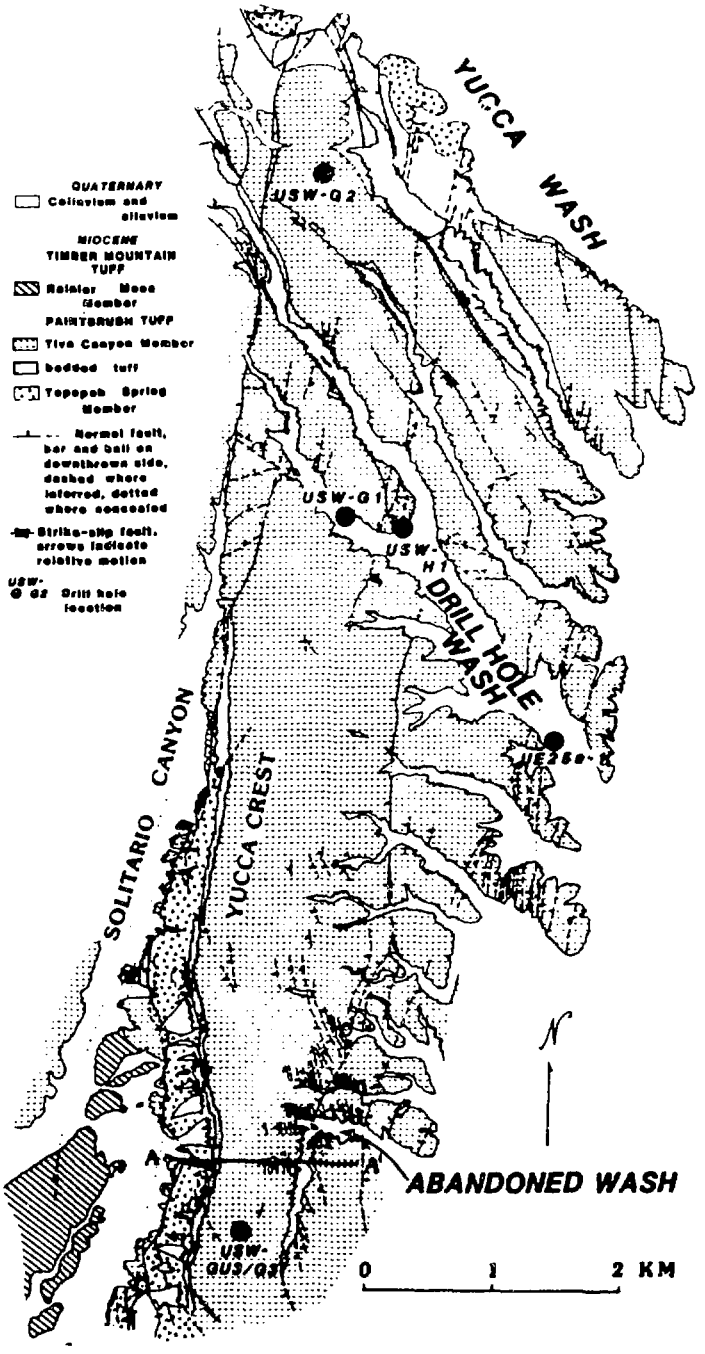

Figure 11. Detailed fault pattern at Yucca Mountain. Faults in the Abandoned Wash area are mapped only on south-facing slopes where exposures are favorable. Attitudes of primary foliation and detailed zones within the Tiva Canyon and Topopah Spring Members are not shown on this figure because of space limitations. Examples of foliation attitudes in the Abandoned Wash area are given in Figure 12.

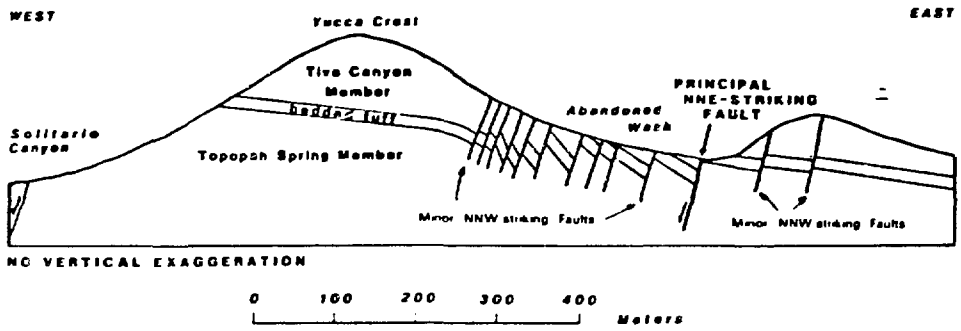

Figure 12. Structure section across Yucca Crest and Abandoned Wash showing the nature of the increase in foliation attitudes toward a north-northeast-striking normal fault and apparent dip-slip movement on representative north-northwest-striking faults.

outcrop is continuous along short traverses in the Tiva Canyon Member, fracture densities are about 6 to 8/unit m^3 measured along the lower lithophysal-clinkstone contact in densely welded tuff. In contrast, fracture densities in the range of only 2 to 4/unit m^3 were observed in the Tiva Canyon Member along the long traverses. Two factors contribute to the apparently lower fracture densities on long traverses. First, the long traverses (one just north of Abandoned Wash and one just south of Drill Hole Wash) were made, by necessity, across outcrop of moderately welded caprock, in addition to the more densely welded zone in the central portion of the Tiva Canyon Member; fractures are considerably more abundant in densely welded tuff than in moderately welded tuff. Both of these long traverses are represented by two rose diagrams, one for the east half and one for the west half; the east halves of these long traverses were made in regions more extensively underlain by moderately welded tuff. Second, by necessity the long traverses were made in part over zones extensively covered with talus; talus preferentially covers gullies which are zones expected to contain high fracture densities. The observation that north-facing slopes, which have more extensive cover, have only about half the fracture densities of the corresponding south-facing slopes, supports this conclusion (fracture densities are calculated only for the fraction of traverse with good exposure). These factors suggest that the most reliable fracture densities are those measured along short traverses, where both maxiumum exposure and uniform stratigraphic interval can be found. The number of variables that cannot be quantified and are inherent to the measure of fracture densities measured along traverses

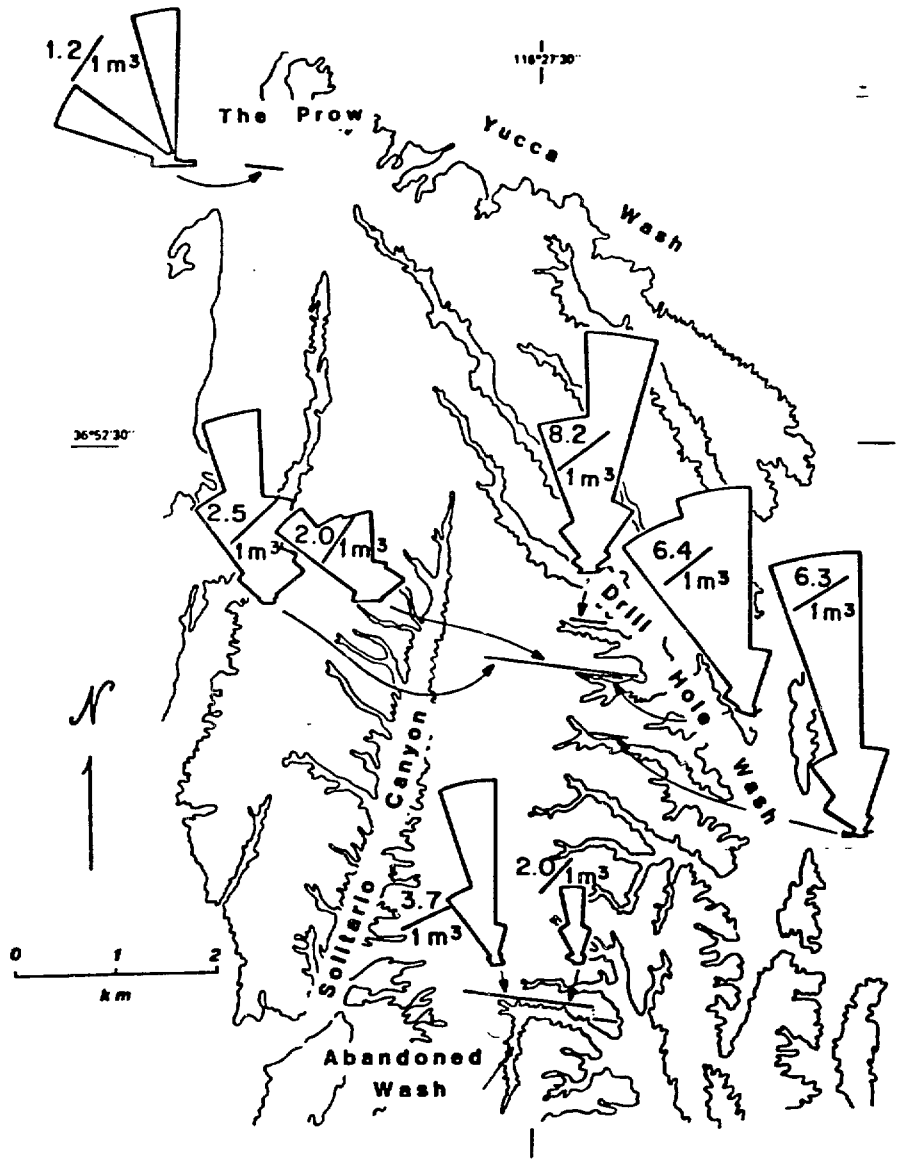

Figure 13. Rose diagrams of the fracture strikes encountered along traverses essentially perpendicular to the average fracture attitude. Five traverses were made in the Tiva Canyon Member, two longer traverses and three shorter traverses. One of the two longer traverses (A) was made south of Drill Hole Wash and the other (B) was made just north of Abandoned Wash. The northernmost of the traverses was made in the tuffaceous beds of Calico Hills. The outline of Yucca Mountain is the Tertiary volcanic rock contact with Quaternary alluvium and colluvium.

suggest that minor differences in fracture densities are not significant.

As mentioned above, the abundance of fractures is a function of both tectonic stresses and cooling stresses. Because nonwelded ash-flow tuffs and bedded tuffs have not been subjected to the stresses related to thermal contraction during cooling, the abundance of fractures in nonwelded tuff might represent exclusively the abundance of tectonic fractures, and the difference between abundance of fractures in welded and nonwelded tuffs might represent the abundance of cooling fractures. This logic breaks down, however, by observation that only a very small portion of the fractures in the rose diagrams of Figure 13 can be assigned to random cooling fractures. The vast majority, therefore, must be tectonically induced. Thus, there is a large difference between the number of tectonic fractures in nonwelded and welded tuffs. Nonwelded tuffs, therefore, have rock mass physical properties that respond to a tectonic stress by formation of relatively few fractures, whereas, welded tuffs have physical properties that respond the the same tectonic stress by formation of more numerous fractures. This conclusion is confirmed by the constant dominant strike of these fractures throughout the mountain, indicating that most of the fractures are of tectonic origin.

5) Dominant fracture strikes are essentially parallel to the north-northwest-striking (about N. 15° W.) faults in the region near Abandoned Wash. Northeast of Drill Hole Wash, however, the north-northwest-striking fractures distinctly intersect the northwest-trending washes and associated strike-slip fault traces. The relationship between the north-northwest-striking fractures and the northwest-striking stike-slip faults is not yet understood, but the 30° angle between them suggests that the fractures may be riedel shears or tension fractures.

6) At numerous localities, slickensides on north-northwest- and northwest-striking faults are nearly horizontal, characteristic of strike-slip motion. In contrast, slickensides on north- to north-northeast-striking faults in the southern and central portions of Yucca Mountain, and particularly those faults that strike in a more north to north-northwest direction, locally concentrated near Yucca Wash, have down-dip attitudes, characteristic of normal fault motion. On two faults with near horizontal slickensides, chattermarks are present. Chattermarks form hairline crescent-shaped fractures [31-32] that are commonly found on glaciated rock surfaces and less commonly on shallow faults. The focus points or noses of the crescents point in the relative direction of movement of the rock face that contains the chattermarks. In both cases on Yucca Mountain,

right-lateral strike-slip motion is unambiguously indicated. Although the magnitude of strike-slip displacement is commonly too small to be measured, at one locality west of drill hole USW-G2, a 10- to 30-m right-lateral offset in the outcrop pattern at the base of the Tiva Canyon Member was measured (Figure 11).

In addition to the structural features described above, there are several characteristics of fractures, such as fracture aperture, vein mineralogy, and extent of vein filling that are also very critical for a complete understanding of fracture control on hydrology. Unfortunately, surface weathering processes and drilling disturbances preclude observation of undisturbed fracture apertures. Also the mineralogy and extent of veins in fractures is so highly variable that generalizations should be avoided. Probably, the cumulative effect of both fracture aperture and mineral filling is best measured by empirical hydrologic testing.

Correlation of Structure with Physical Property Stratigraphy

Based upon fracture attitudes and densities measured downhole from both unoriented cores, oriented cores, and downhole televison video tapes, an impressive positive correlation between degree of welding and density of fractures in core recovered from drill hole USW-GU3/G3 is shown in Figure 14. The density of fractures has been corrected for the attitude relative to the core axis as described above, and is expressed as the number of fractures/unit m^3. To depths of 940 m, the more elastic (lower Young's Modulus or stiffness) zeolitized nonwelded and partially welded tuffs [27] have as few as 1 to 3 fractures/unit m^3, whereas the more brittle (higher Young's modulus or stiffness) densely welded tuffs typically have 20 to 40 fractures/unit m^3. Fracture densities in core from drill holes USW-G2 and -G1 are somewhat lower, but the overall patterns are similar. Below 940 m, the abundance of fractures decreases by nearly an order of magnitude in core from USW-GU3/G3. Further investigations are being conducted to determine whether this decrease in fracture density is related to the more ductile behavior at higher confining pressures, to the somewhat more altered state of these more deeply buried tuffs, or merely to a change in tectonic style, independent of depth. The degree of welding of the more extensively welded tuffs below 940 m falls more into the moderately welded range rather than the densely welded range, and the degree of alteration is significantly greater. Although there is an expected decrease in fracture

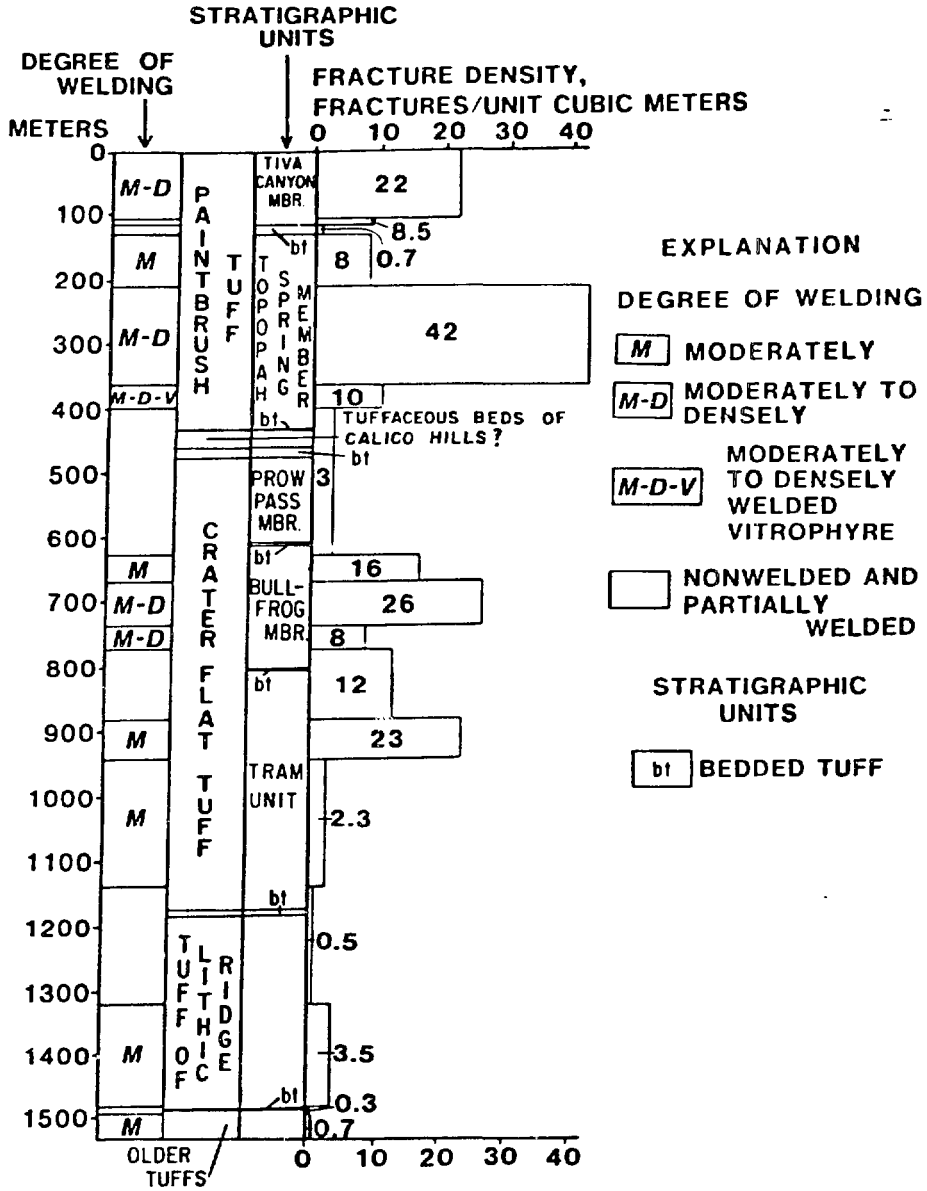

Figure 14. Density of fractures compared to physical-property stratigraphy expressed by differences in degree of welding in drill hole USW-GU3/G3 shown in Figure 4. These fractures include only mineralized cracks or cracks that have evidence of shear such as breccia, gouge, or slickensides. The density of fractures has been calculated per unit m^3. The density of fractures at drill holes USW-G1 and -G2 is somewhat lower than at -GU3/G3, but the overall correlation with degree of welding is similar.

density related to these factors, the decrease from 23 fractures/unit m^3 in the moderately welded Tram unit above 940 m to 2.3 fractures/unit m^3, also in moderately welded Tram unit, below 940 m requires an explanation other than a change in degree of welding.

The densities of fractures in densely welded tuff measured in core (20 to 40/unit m^3) do not correlate well with densities measured in well-exposed outcrops of densely welded tuff (6 to 8/unit m^3). In all probability, fractures are both more readily seen in core, and the mechanical disturbance of coring enhances parting along abundant hairline aperture fractures not visible on surface exposures. The dominant northwest strike of the fractures measured in oriented core (N. 15° W., 75° SW., Figure 15) from drill hole USW-GU3/G3 (R. B. Scott, USGS and Mayra Castellanos, F&S, written commun., 1982), however, does agree well with those measurements on the surface (Figure 13). Also the average fault attitude in this core (N. 21° W., 73° SW.) is similar to the north-northwest-striking faults mapped on the surface in the vicinity of Abandoned Wash (Figure 11).

Drill-Hole Deviation

Drill holes on Yucca Mountain tend to deviate naturally from vertical, almost uniformly to the southwest and west (Figure 16). Holes USW-G1, USW-H1, and UE25a-1, all within Drill Hole Wash, trend S. 30° W. to S. 60° W., to a depth of over 1 km, essentially perpendicular to Drill Hole Wash. Holes USW-G2 and USW-G3, in contrast, trend slightly south of west, from S. 80° W. to S. 83° W. Because Drill Hole Wash appears to be controlled, at least in part, by fracture and fault systems that strike nearly parallel to the wash and dip steeply (60°-90°) toward the southwest, the uniform drill-hole deviation direction may also be controlled if the core bit tends to follow the path of least resistance down near-vertical fractures and faults. However, within the Yucca Mountain block, away from influence of the structures in the washes, the trend of dip of dominant fractures and faults is only slightly south of west; apparently the drill-hole deviation follows a similar trend and plunge. Thus, drill-hole deviation directions appear to be sensitive indicators of anisotropic mechanical properties of the rock, in this case, fracture attitudes.

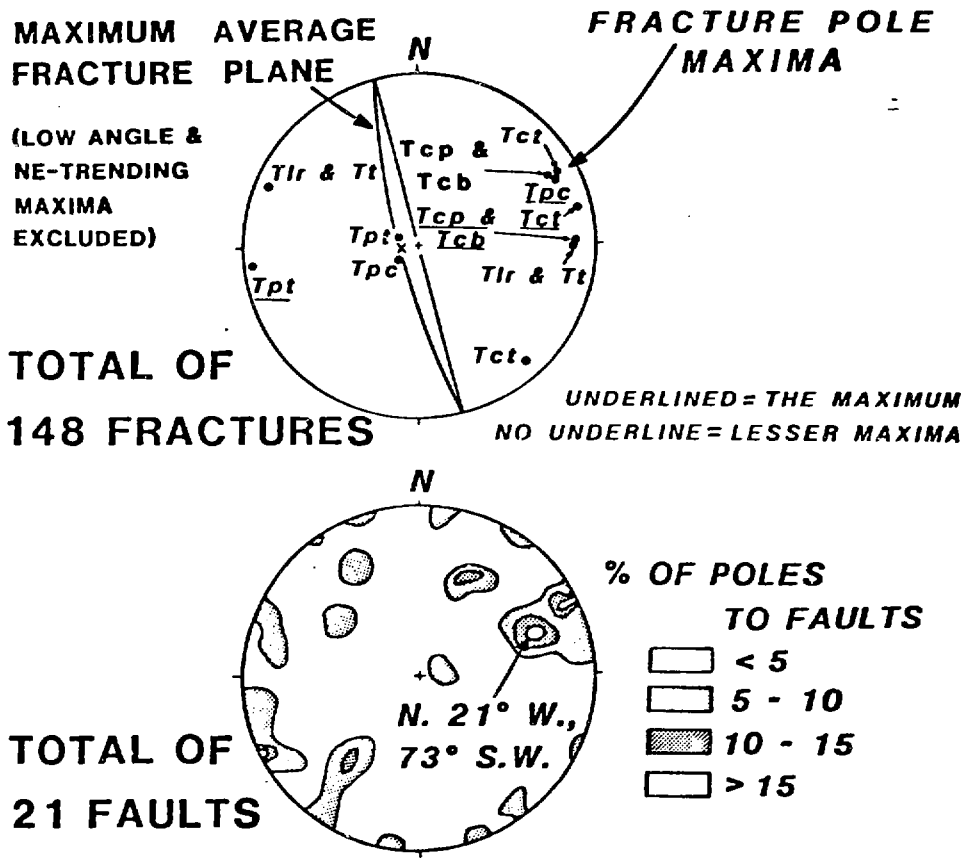

Figure 15. Lower hemisphere poles to attitudes of average fractures and faults measured in oriented core from USW-GU3/G3 and corrected for drilling deviation (R. B. Scott, USGS, and Mayra Castellanos, F&S, written commun., 1982). The average fracture plane (N. 15° W., 81° SW.) was calculated in the upper diagram by averaging the stereonet maxima for all the poles to fracture planes from each stratigraphic unit. Also in the upper diagram, the averaged direction of drill hole deviation is shown by the X. The stereonet maximum for the fault attitude (N. 21° W., 73° SW.) is shown in the lower diagram. The Tiva Canyon Member (Tpc) and Topopah Spring Member (Tpt) are part of the Paintbrush Tuff. The Prow Pass Member (Tcp), Bullfrog Member (Tcb), and Tram unit (Tct) from the Crater Flat Tuff. Tlr symbolizes the tuff of Lithic Ridge and Tt symbolizes the older unnamed tuffs.

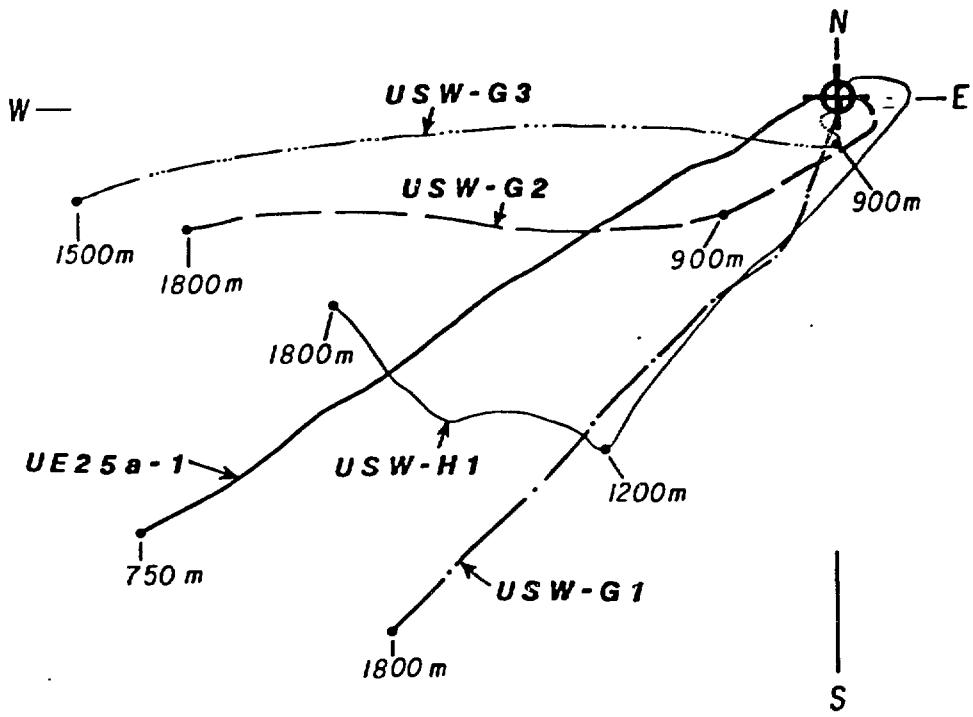

Figure 16. Drill-hole deviation directions on Yucca Mountain. Note that no horizontal scale is given because the amount of lateral deviation varies. Line lengths are normalized to represent percent of horizontal deviation.

DISCUSSION

Regional Structural Framework

Although the dominant Tertiary faults in the NTS are north-northeast-striking, Basin and Range style, normal faults [18,21], Carr [11] reported a significant overprint of strike-slip fault displacement, particularly left-lateral displacement on the north-northeast-striking faults. Carr did not observe right-lateral strike-slip displacement on northwest-striking faults elsewhere in the NTS; he concluded that strike-slip displacement is not expected because these faults would be under compression under the current stress regime. However, on Yucca Mountain, evidence of right-lateral displacement exists on north-northwest-striking faults south of Drill Hole Wash and on northwest-striking faults north of Drill Hole Wash. Major movement on these fault systems and the north-northwest-striking fracture

system do not appear to affect the Rainier Mesa Member at Yucca Mountain; thus, the probable age of this fracturing and faulting is between the age of the faulted Tiva Canyon Member, about 12.5 m.y., and the age of the Rainier Mesa Member, about 11.3 m.y. From a regional perspective, the general attitude, sense of displacement, and age of these northwest-striking features are very similar to those features of regional strike-slip zones including the Las Vegas Valley and Walker Lane shear zones (Figure 17) [33-34]. A

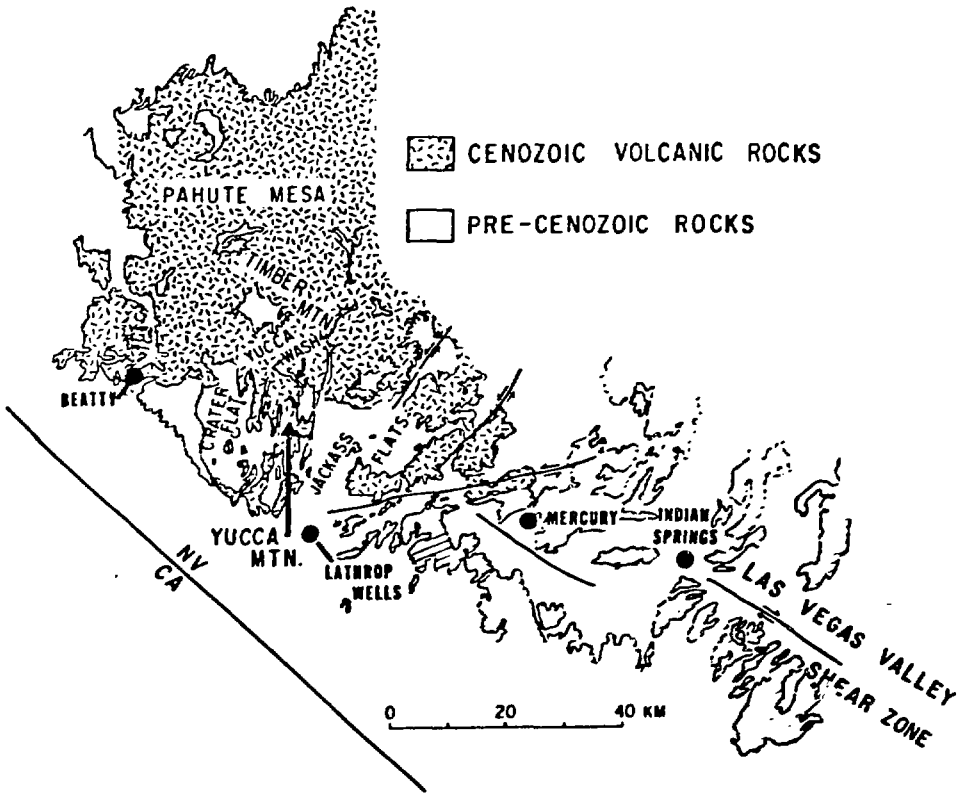

Figure 17. Location of the Las Vegas Valley shear zone [21] relative to the Yucca Mountain region. Note the parallelism of the shear zone and the elongation of Yucca Wash.

physical extension of the Las Vegas Valley shear zone itself to Yucca Mountain seems unlikely, even though most of the rocks exposed in the intervening area postdate regional shear zone activity [36-37]. A diffuse zone of right-lateral stike-slip with small displacements is probably more likely, but very difficult to recognize in the field.

The major observable displacement on faults in the Abandoned Wash area along both the numerous north-northwest-striking faults and the major north-northeast-striking

block-bounding fault appears to be dip-slip and, as a result, that area appears to have experienced significant extension. The general increase in eastward dip of the down-faulted blocks west of the major block-bounding fault in this area is very similar to the roll-over features or "reverse drag" observed along growth faults in the Gulf Coast region and normal faults in the Colorado Plateau region [38-39]. If the features at Yucca Mountain are of similar origin, then the dips of major block-bounding faults under Yucca Mountain probably decrease at some as yet unobserved depth in a manner similar to those of listric growth faults on the Gulf Coast, as Wernicke and Burchfiel [40] have recently suggested for extensional systems of the Great Basin. Where large vertical displacements (about 100^{+} m) occur, such as along the eastern margin of Solitario Canyon (Figure 11), chaotic zones of breccia and extremely irregular fault blocks including overturned sequences are present on the hanging-wall side of the fault. Presumably these chaotic zones develop where movement along the listric fault creates a significant gap at the head of the fault and blocks collapse in a disorganized fashion to fill a developing gap. Abandoned Wash is an example of smaller vertical displacement between major blocks (about 25 m), and therefore, smaller gap formation on the hanging-wall of the listric system. In this case, the fractured rock in the roll-over structure has retained coherent block-to-block contact with the major normal fault. Drag on these surfaces produces the offset observed; in essence, this is a brittle response to drag along the major fault (Figure 12). These features further suggest that the brittle behavior seen in the Tiva Canyon and Topopah Spring Members at the surface probably goes through a transition at depth to more ductile behavior where these faults begin to flatten. The abundant fractures characteristic to depths of about 1 km depth and the mechanical contrast that produces uniform drill-hole deviation both reinforce the concept that the exposed portion of Yucca Mountain is within the upper brittle behavior region. Data do not exist at present to predict the depth of the transition to more ductile behavior, but the presence of "reverse drag" dips should persist to at least 1 km.

An alternative interpretation to the listric fault hypothesis given above is that the steeper foliation attitudes observed in Abandoned Wash are related to rotation by a component of strike-slip displacement (W. J. Carr, oral commun., 1982). In the absence of more discriminatory evidence, the listric fault explanation appears most likely.

Conceptual Hydrologic Model

Direct hydrologic investigations of the unsaturated zone at Yucca Mountain are underway but are too preliminary to construct an an empirical model of the hydrology at this early stage. However, knowledge of the gross physical property stratigraphy combined with a three-dimensional model of fracture and fault attitudes and densities, in conjunction with regional hydrologic observations and regional conceptual models of the hydrology of ash-flow tuffs [5,7,22], does allow construction of a very simple conceptual hydrologic model at Yucca Mountain.

Limited physical-property data [25] are available from core samples from the unsaturated zone at Yucca Mountain. These data include matrix hydraulic conductivities that fall within the ranges listed in Table I, for the most part (2×10^{-10} to 3×10^{-9} cm/s for the densely welded Tiva Canyon Member, 8×10^{-10} to 2×10^{-7} cm/s for the densely welded Topopah Spring Member, and 4×10^{-9} to 1.5×10^{-6} cm/s for the underlying zeolitized nonwelded ash-flow and bedded tuffs). Also these data include natural, saturated, and dry bulk densities, from which the degree of saturation was calculated. The range of saturation of the welded Tiva Canyon Member samples is 33 to 50 percent, the underlying nonwelded ash-flow and bedded tuffs is 61 to 90 percent, the welded Topopah Spring Member is 17 to 91 percent, and the underlying nonwelded ash-flow and nonwelded tuffs is 82 to 100 percent. Even below the static water level, within the deepest interval listed above, the range of saturation is between 82 and 100 percent. The lower densities, higher porosities, higher degree of saturation, and higher surface areas of the nonwelded tuffs suggest that they may act as temporary capillary barriers (W. E. Wilson, USGS, oral commun., 1982), but the unsaturated zone has probably reached a steady-state flow such that each layer is as saturated as possible with a balance of capillary forces, gravity, and back pressure of trapped gases. Thus, any pulse of water migrating through the rock would be in excess of what the rock can absorb, and therefore, would eventually pass through these nonwelded layers.

The generalized and greatly simplified cross section drawn through the unsaturated zone in Yucca Mountain in Figure 18 assumes the more welded portions of the Tiva Canyon and Topopah Springs Members to be highly transmissive units with high effective conductivities. Because the fracture densities in lithophysal zones in the densely welded tuffs of the Tiva Canyon Member (14 to 22 fractures/unit m^3) do not appear to differ appreciably from those within non-lithophysal densely welded zones (22 to 26 fractures/unit

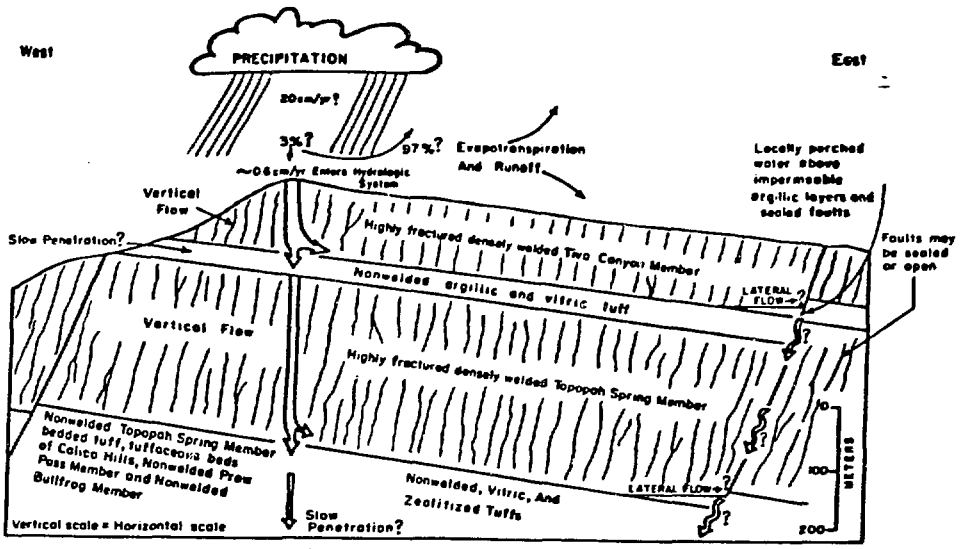

Figure 18. Conceptual hydrologic model of Yucca Mountain, assuming a positive net recharge for the mountain. Determination of vertical and possible horizontal rates of transmission of recharge through densely and moderately welded Tiva Canyon and Topopah Spring Members and through less welded vitiric, argillic and zeolitized tuffs awaits hydrologic testing specifically designed for the unsaturated zone. If faults are locally sealed, they may create local perched water tables, but if they are open, the faults may rapidly transmit water.

m^3), it is assumed that lithophysal zones will have hydrologic properties similar to densely welded nonlithophysal zones. The abundance of cavities in lithophysal zones may increase the conductivities locally where the fractures interconnect with cavities. Between and below these more welded portions of the Tiva Canyon and Topopah Spring Members are bedded tuffs and nonwelded to partially welded ash-flow tuffs that have few fractures. Where these less welded units are vitric, they may act as "leaky aquitards", the term used by Winograd and Thordarson [5], because they have relatively high matrix conductivities. However, where these bedded tuffs and less welded tuffs are altered to clays and zeolites [29], their matrix conductivities are considerably lower than those of vitric tuffs, and they have low hydraulic conductivities because of the low fracture densities. These less welded altered tuffs may have the capacity to act as capillary barriers because of the lower

hydraulic conductivities. Observations by Thordarson [22], at Rainier Mesa northeast of Yucca Mountain in a similar setting on the NTS, indicate that perched water does occur above locally saturated zeolitized tuffs within the unsaturated zone.

Of the small annual precipitation that occurs in this arid region (less than 20 cm/yr in the Jackass Flats drainage basin), less than about 3 percent is estimated [40] to enter the hydrologic system as recharge on a basin-wide average. Because Yucca Mountain stands roughly 400 m higher than Jackass Flats, it is assumed here that a positive recharge does occur at 3 percent of 20 cm/yr (actual measurements of precipitation or recharge on Yucca Mountain have not been made). Thus, roughly 0.6 cm of water would enter the system annually and would be transmitted through the highly fractured zone of the densely welded portion of the Tiva Canyon Member. Where the water encounters vitric tuffs below the welded Tiva Canyon Member, the water may tend to be temporarily absorbed in the porous nonwelded tuffs above the Topopah Spring welded tuffs; however, pore sizes in vitric tuff are considerably greater than those in zeolitized tuffs, and eventually water would penetrate these vitric layers. On the other hand, where these nonwelded vitric layers are clay-rich and have low conductivities, they may become essentially water saturated, and may inhibit vertical flow sufficiently to locally or temporarily pond water, producing perched water tables above the Topopah Spring Member. After vertical passage through densely welded zones and the vitrophyre of the Topopah Spring Member, the water would encounter the deeper zone of nonwelded tuffs. Although these tuffs are extensively zeolitized, the zeolitization is discontinuous, particularly toward the southern portion of Yucca Mountain where the water table is deeper and the tuffs are still vitric (R. B. Scott, USGS, and Mayra Castellanos, F&S, written commun., 1982). Whether zeolitization is a requirement and whether argillization can create similar conditions conducive to perched water tables in ash-flow tuffs on Yucca Mountain is not known at the present time. Direct evidence to suggest that perched water exists within Yucca Mountain has not been found, but wet areas on the surface exist above zeolitized tuffs along the steep walls of Yucca Wash, indirectly suggesting that some perched water may be present along this horizon. Such hydrologic barriers may also cause limited lateral movement of water down dip (east and southeast) of the stratigraphic boundary and along the major fracture attitude (south-southeast and southeast). This general southeast direction would be essentially parallel to flow directions down the hydrologic gradient (F. E. Rush, USGS, oral commun., 1982).

Faults may either be sealed by formation of fault gouge or secondary mineralization, forming relatively nontransmissive barriers and creating local perched water, or they may be open, highly transmissive paths through both nonwelded tuffs and the highly transmissive Topopah Spring Member. Eventually that portion of the recharge that moves vertically must permeate the nonwelded base of the Topopah Spring Member, the nonwelded, zeolitized tuffaceous beds of Calico Hills, various zeolitized and argillized bedded tuffs, and the nonwelded to partially welded zeolitized Prow Pass Member before reaching the static water level, unless a fault acts as a short-circuit conduit. Faults may be highly impermeable in general, especially in nonwelded zones but observations of open faults in core to depths greater than the static water level suggest that unless detailed empirical data exist to support the contention that a specific fault is impermeable, high permeabilities should be considered as possible, at least locally.

The validity of the simplified conceptual model shown in Figure 18 will be tested as empirical data are gathered. At present the model can best be used to design future hydrologic testing and to recognize areas where additional structural and hydrologic data are needed. Obviously, the reality of hydrologic flow within the unsaturated zone under Yucca Mountain is far more complex than the model is capable of suggesting; a number of unknown factors will have to be investigated (R. K. Waddell, USGS, oral commun., 1982): What is the annual average precipitation and recharge at Yucca Mountain? What is the relation between recharge flux and lithophysal zones? How does water flow through layers of variable degrees of saturation, degrees of welding, and variable densities of fracturing? Do fractured densely welded tuffs have fracture conductivity as the dominant mode and nonwelded tuffs have matrix conductivity as the dominant mode of water flow? How much smaller are matrix and effective conductivities in the unsaturated zone than in the saturated zone? At what rates does water flow through rocks with these variable characteristics? To what degrees do porous layers act as capillary barriers? Until these and other problems are addressed, a more realistic and complex model is difficult to produce. The viability of the unsaturated zone under Yucca Mountain as a nuclear waste repository will depend, in part, upon reaching an understanding of the complex physical process of fluid transmission in the unsaturated zone of Yucca Mountain.

CONCLUSIONS

Determination of the viability of nuclear waste disposal in the unsaturated zone of ash-flow tuffs at Yucca Mountain is highly dependent upon a three-dimensional evaluation of physical, structural, and hydrologic properties of the rock mass.

A) Listed below are four major conclusions reached from the investigation of rock mass physical properties.

A1) The physical-property stratigraphy in tuffs at Yucca Mountain is defined principally by layers of contrasting degrees of welding, bulk density, and porosity. Physical-property stratigraphy, rather than conventional petrologic stratigraphy, must be used to characterize the inhomogeneous and layered rock body.

A2) Within densely welded portions of the Tiva Canyon and Topopah Spring Members of the Paintbrush Tuff, the density of fractures measured on core 6.25 cm in diameter is commonly 20 to 40 fractures/unit m^3. Detailed surface traverses indicate a lower fracture density for this rock type, in the range of 6 to 8 fractures/unit m^3.

A3) Partially welded and nonwelded tuffs have considerably fewer fractures than welded tuffs, commonly as few as 1 to 3 fractures/unit m^3. Also they are commonly altered to clays and zeolites.

A4) Although a number of surface characteristics that create mappable zonations (such as the clinkstone, hackly, and columnar zones) appear to be related to detailed devitrification fabrics, the fracture density appears to be relatively independent of this variable. Also, the lithophysal content and grain density do not appear to appreciably affect the fracture density.

B) Listed below are four major conclusions reached from the investigation of the structural geology of the unsaturated zone.

B1) The dominant strike of fractures in both welded and nonwelded tuffs, as measured in both outcrop and core, is about N. 15° W.. This indicates that most of the observed fractures are tectonically induced, as a random distribution of fracture strikes should result from contraction-induced jointing.

B2) The small-displacement north-northwest strikes of faults in the Abandoned Wash vicinity in the southern portion of Yucca Mountain are parallel to the dominant strike of fractures. However, north of Drill Hole Wash, faults appear to be more nearly parallel to the washes, about N. 25° W. to N. 40° W.

B3) Several of the northwest-striking minor faults have slickensides and chattermarks compatible with right-lateral, strike-slip motion. This attitude and sense of displacement suggests that a genetic relation between the regional Las Vegas Valley and Walker Lane shear systems and these local Yucca Mountain structures may exist. This movement appears to postdate the Tiva Canyon Member of the Paintbrush Tuff (12.5 my old) but predate the Rainier Mesa Member (11.3 my old) of the Timber Mountain Tuff.

B4) On the hanging-wall side of several major north-northeast-striking normal faults in Yucca Mountain, the increase in foliation dip may be analogous to roll-over structures associated with listric faults. Also, the closely-spaced, small-displacement normal faults in Abandoned Wash may result from drag along the major faults. The major movement on normal faults on Yucca Mountain occurred within the same time interval as the strike-slip faults mentioned above.

C) The conclusions reached from physical-property and structural investigations of Yucca Mountain allow the construction of the following preliminary conceptual hydrologic model based upon the fundamental assumption that a net positive recharge occurs on the mountain.

C1) The uniform high fracture density and brittle character of densely welded tuffs indicate that, in spite of their low matrix conductivities, their effective hyraulic conductivities are uniformly high; this conclusion is supported by limited in situ hydraulic conductivity measurements within the saturated zone of the densely welded Topopah Spring Member near Yucca Mountain [5]. Thus, in the unsaturated zone, the fractures in densely welded tuffs should readily transmit fluids, provided a maximum or steady-state degree of saturation of the rock matrix exists; that is, assuming the rock matrix has already absorbed all the water it can retain in the unsaturated zone.

C3) The low fracture density and low matrix hydraulic conductivities of zeolitized or argillized nonwelded tuffs suggests that they should serve as potential aquitards below the water table [5] and as infiltration barriers within the unsaturated zone.

C4) The relatively high matrix conductivities of nonwelded vitric tuffs indicates that these tuffs should serve as relatively permeable zones, even in the absence of fracturing [5], but the rate of transmission of flow in the unsaturated zone may be inhibited to a degree by possible capillary action of these porous tuffs.

C5) Although the vast majority of recharge probably moves vertically, limited lateral flow associated with perched water may occur above relatively impermeable zeoli-

tized or argillized nonwelded zones. Even though Thordarson [22] did not find evidence to support significant lateral flow in a similar setting in the unsaturated zone under Rainier Mesa northeast of Yucca Mountain, he did find perched water above highly zeolitized tuffs there. The east to southeast dip and north-northwest-striking fractures on Yucca Mountain, absent at Rainier Mesa, would be conducive to lateral flow of perched water in an east or southeast direction.

C6) Development of this hydrologic model has identified several areas where important fundamental data are needed for an understanding of the hydrology of the unsaturated zone: a) What is the range of annual precipitation on Yucca Mountain and what is the range of annual recharge? b) Is the dominant mode of transmission of fluids along fractures in densely welded tuffs, but within the rock matrix in zeolitized or argillized nonwelded tuffs and in vitric nonwelded tuffs? c) How do rates of fluid transmission in the unsaturated zone differ from those in the saturated zone within similar rocks? d) Do porous vitric tuffs act as capillary barriers in a steady state system? e) Does limited lateral flow occur and does perched water exist? f) Do specific faults within Yucca Mountain act as hydrologic barriers or as highly permeable hydrologic short circuits?

ACKNOWLEDGMENTS

As in any attempt to correlate several disciplines, much credit belongs to numerous colleagues: In addition to formal USGS technical reviews, numerous USGS hydrologists including Ike Winograd, Bill Wilson, Rick Waddell, Merrick Whitfield, and Jim Robison, have freely given advice. Mike Carr has also provided a particularly valuable informal geologic review. Barry Swartz of SNL transmitted the physical-property measurements for this work and Larry Teufel, also of SNL, gave advice concerning the behavior of these ash-flow tuffs under stress. Judy Brandt and Byron Cork, among others of Fenix and Scisson, provided field assistance. Finally Jim Mercer's understanding of interminable delays in submitting the manuscript is deeply appreciated.

REFERENCES

1. Eckel, E. B., ed. "Nevada Test Site," *Geol. Soc. Amer. Mem. 110*: 290p. (1968).

2. Winograd, I. J. "Radioactive waste disposal in thick unsaturated zones," *Science 212*: 1457-1464 (1981).
3. Christiansen, R. L., and Lipman, P. W. "Geologic map of the Topopah Spring NW quadrangle, Nye County, Nevada," *U. S. Geol. Survey Geol. Quad. Map GQ-444*, scale 1:24,000 (1965).
4. Lipman, P. W., and McKay, E. J. "Geologic map of the Topopah Spring SW quadrangle, Nye County, Nevada," *U. S. Geol. Survey Geol. Quad. Map GQ-439*, scale 1:24,000 (1965).
5. Winograd, I. J., and Thordarson, William " Hydrogeologic and hydrochemical framework, south-central Great Basin, Nevada-California, with special reference to the Nevada Test Site," *U. S. Geol. Survey Prof. Paper 712-C*: C1-C126p. (1975).
6. Smith, R. L. "Zones and zonal variations in welded ash-flows," *U. S. Geol. Survey Prof. Paper 345-F*: F149-F154 (1960).
7. Winograd, I. J. "Hydrogeology of ash flow tuff: a preliminary statement," *Water Resources Research 7*: 994-1006 (1971).
8. Byers, F. M., Jr., Carr, W. J., Orkild, P. P., Quinlivan, W. D., and Sargent, K. A. "Volcanic suites and related cauldrons of Timber Mountain-Oasis Valley caldera complex, southern Nevada," *U. S. Geol. Survey Prof. Paper 919*: 70p. (1976).
9. Christiansen, R. L., Lipman, P. W., Orkild, P. P., and Byers, F. M., Jr. "Structure of the Timber Mountain caldera, southern Nevada, and its relation to Basin-Range structure," *U. S. Geol. Survey Prof. Paper 525B*: B43-B48 (1965).
10. Christiansen, R. L., Lipman, P. W. Carr. W. J., Byers, F. M., Jr., Orkild, P. P., and Sargent K. A. "Timber Mountain-Oasis Valley caldera complex of southern Nevada," *Geol. Soc. Amer. Bull. 88*: 943-959 (1977).
11. Carr, W. J. "Summary of tectonic and structural evidence for stress orientation at the Nevada Test Site," *U. S. Geol. Survey Open-File Rpt. 74-176*: 53p. (1974).
12. Spengler, R. W., Byers, F. M., Jr., and Warner, J. B. "Stratigraphy and structure of volcanic rocks in drill Hole USW-G1, Yucca Mountain, Nye County, Nevada," *U. S. Geol. Survey Open-File Rpt. 82-1349*: 36p. (1981).
13. Spengler, R. W., Muller, D. C. and Livermore, R. B. "Preliminary report on the geology of drill hole UE25a-1, Yucca Mountain, Nevada Test Site," *U. S. Geol. Survey Open-File Rpt. 79-1244*: 43p. (1979).

14. Spengler, R. W., and Rosenbaum, J. G. "Preliminary interpretations of results obtained from boreholes UE25a-4, -5, -6, -7, Yucca Mountain, Nevada Test Site," *U. S. Geol. Survey Open-File Rpt. 80-929*: 35p. (1980).
15. Snyder, D. B., and Carr, W. J. "Preliminary results of gravity investigations at Yucca Mountain and vicinity, southern Nye County, Nevada," *U. S. Geol. Survey Open-File Rpt. 82-701*: 36p. (1982).
16. Carr, W. J. "Volcano-tectonic history of Crater Flat, southwestern Nevada, as suggested by new evidence from drill hole USW-VH-1 and vicinity," *U. S. Geol. Survey Open-File Rpt. 82-457*: 23p. (1982).
17. Lipman, P. W., Christiansen, R. L., and O'Connor, J. T. "A compositionally zoned ash-flow sheet in southern Nevada," *U. S. Geol. Survey Prof. Paper 524-F*: F1-F47 (1966).
18. Stewart, J. H., and Carlson, J. E. "Geologic map of Nevada," *U. S. Geol. Survey: scale 1*:500,000 (1978).
19. Armstrong, R. L. "Sevier orogenic belt in Nevada and Utah," *Geol. Soc. Amer. Bull. 79*: 429-458 (1968).
20. Barnes, Harley, and Poole, F. G. "Regional thrust fault system in Nevada Test Site and vicinity" *in* Nevada Test Site, *Geol. Soc. Amer. Memoir 110*: 233-238 (1968).
21. Ekren, E. B., Rogers, C. L., Anderson, R. E., and Orkild, P. P. "Age of Basin and Range normal faults in Nevada Test Site and Nellis Air Force Range, Nevada," *in* Nevada Test Site, *Geol. Soc. Amer. Memoir 110*: 247-250 (1968).
22. Thordarson, W. "Perched ground-water in zeolitized-bedded tuff, Rainier Mesa and vicinity, Nevada Test Site, Nevada," *U. S. Geol. Survey Open-File Rpt. TEI-862*: (1965).
23. Blankennagel, R. K., and Wier, J. E. "Geohydrology of the eastern part of Pahute Mesa, Nevada Test Site, Nye County, Nevada," *U. S. Geol. Survey Prof. Paper 712-B*: B1-B34 (1973).
24. Young, R. A. "Water supply for the Nuclear Rocket Development Station at the U. S. Atomic Energy Commission's Nevada Test Site," *U. S. Geol. Survey Water Supply Paper 1938*: 19p. (1972).
25. Anderson, L. A. "Rock property analysis of core samples from the Yucca Mountain UE25a-1 borehole, Nevada," *U. S. Geol. Survey Open-File Rpt. 81-1338*: 36p. (1981).

26. Lappin, A. R., Van Buskirk, R. G., Enniss, D. O., Butters, S. W., Prater, F. M., Muller, C. B., and Bergosh, J. L. "Thermal conductivity, bulk properties, and thermal stratigraphy of silicic tuffs from the upper portions of hole USW-G1; Yucca Mountain, Nye County, Nevada," *SAND81-1873, Sandia National Laboratories, Albuquerque, NM*: 78p. (1982).
27. Olsson, W. A., and Jones, A. K. "Rock mechanics properties of volcanic tuffs from the Nevada Test Site," *SAND80-1453, Sandia National Laboratories, Albuquerque, NM*: 54p. (1980).
28. Lappin, A. R. "Bulk and thermal properties of the functional tuffaceous beds in holes USW-G1, UE25A#1, and USW-G2, Yucca Mountain, Nevada," *SAND82-1434, Sandia National Laboratories, Albuquerque, NM*: 62p. (1982).
29. Caporuscio, F., Vaniman, D., Bish, D., Broxton, D., Arney, B., Heiken, G., Byers, F., Gooley, R., and Semarge, E. "Petrology studies of drill cores USW-G2 and UE25b-1H, Yucca Mountain, Nevada," *LA-9255-MS, Los Alamos National Laboratory, Los Alamos, NM*: 111p. (1982).
30. Terzagi, R. D. "Sources of error in joint surveys," *Geotechnique 15*: 287-304 (1965).
31. Chamberlin, T. C. "The rock scorings of the great ice invasions," *U. S. Geol. Survey 7th. Ann. Rpt.*: 218-223 (1885).
32. Johnson, B. C. "Characteristics and mechanics of formation of glacial arcuate abration cracks," *unpubl. Ph.D. dissertation, Penn. State Univ.*: 253p. (1975).
33. Stewart, J. H., Albers, J. P., and Poole, F. G. "Summary of regional evidence for right-lateral displacement in the western Great Basin," *Geol. Soc. Amer. Bull. 79*: 1407-1414 (1968).
34. Guth, P. L. "Tertiary extension north of the Las Vegas Valley shear zones, Sheep and Desert ranges, Clark County, Nevada," *Geol. Soc. Amer. Bull. 92*: 763-771 (1981).
35. Fleck, R. J. "Age and possible origin of the Las Vegas Valley shear zone, Clark and Nye Counties, Nevada," *Geol. Soc. Amer. Abstracts with Programs 2*: 333 (1970).
36. Sargent, K. A. and Stewart, J. H. "Geologic map of the Specter Range NW quadrangle, Nye County, Nevada," *U. S. Geol. Survey Quad. Map GQ-884*: scale 1:24,000 (1971).
37. McKay, E. J. and Williams, W. P. "Geologic map of the Jackass Flats quadrangle, Nye County, Nevada," *U. S. Geol. Survey Quad. Map GQ-368*: scale 1:24,000 (1964).

38. Bruce, C. H. " Pressured shale and related sedimentary deformation: mechanisms for development of regional contemporaneous faults," *Amer. Assoc. Petrol. Geol. Bull. 57*: 878-886 (1973).
39. Hamblin, W. K. "Origin of "reverse drag" on the downthrown side of normal faults," *Geol. Soc. Amer. Bull. 76* 1145-1164 (1965).
40. Wernicke, B. and Burchfiel, B. C. "Modes of extensional tectonics," *Jour. Structural Geol. 4*: 105-115 (1982).
41. Rush, F. E. "Regional groundwater system in the Nevada Test Site area, Nye, Lincoln, and Clark Counties, Nevada," *Nevada Dept. Conservation Natural Resources Reconnaissance Series, Rpt. 54*: 25p (1970).